Effects of Site Response on the Correlation Structure of Ground Motion Residuals

Maryam Motamed

Thesis submitted to the faculty of the
Virginia Polytechnic Institute and State University
in partial fulfillment of the requirements for the degree of

Master of Science
In
Civil Engineering

Adrian Rodriguez- Marek - Chair
Matthew Mauldon
Joseph E. Dove

October 11th, 2013
Blacksburg, Virginia

Keywords: Site response analysis, Correlation coefficient, Ground motion prediction equation

Effects of Site Response on the Correlation Structure of Ground Motion Residuals

Maryam Motamed

ABSTRACT

Seismic hazard analyses require an estimate of earthquake ground motions from future events. These predictions are achieved through Ground Motion Prediction Equations, which include a prediction of the median and the standard deviation of ground motion parameters. The differences between observed and predicted ground motions, when normalized by the standard deviation, are referred to as epsilon (ϵ). For spectral accelerations, the correlation structure of normalized residuals across oscillator periods is important for guiding ground motion selection. Correlation structures for large global datasets have been studied extensively. These correlation structures reflect effects that are averaged over the entire dataset underlying the analyses. This paper considers the effects of site response, at given sites, on the correlation structure of normalized residuals. This is achieved by performing site response analyses for two hypothetical soil profiles using a set of 85 rock input motions. Results show that there is no significant difference between correlation coefficients for rock ground motions and correlation coefficients after considering the effects of site response for the chosen sites.

KEY WORD DEFINITIONS

GMPE: Ground Motion Prediction Equation

PGV: Peak Ground Velocity

PGA: Peak Ground Acceleration

ASI: Acceleration Spectrum Intensity (cm/s)

SI: Spectrum intensity

SA: Spectral Acceleration.

V_{s30}: Shear velocity of the site profile at the top 30 m of soil layer.

ACKNOWLEDGEMENT

I wish to acknowledge all individuals who assisted in completion of this thesis. First, I want to thank my adviser, Dr. Adrian Rodriguez-Marek for his inspiration, guidance, instruction, encouragement and support. His advice and knowledge helped me to complete my studies at Virginia Tech. He enabled me to develop an understanding of the subject and motivated me to complete this research.

Also, I am grateful to my committee members for their continuous support from the beginning of the research to its completion. Sincere appreciation is expressed to the faculty in the Civil Engineering Department and especially geotechnical program at Virginia Tech for providing us with such a nourishing environment that give us the opportunity to grow our knowledge extensively and to prepare us for our professional life.

I also offer my regards and appreciation to my parents and my friends for their support, encouragement, and devotion which motivated me to be successful in my studies at Virginia Tech.
I would not have finished my study and my research if it were not for my mother's love and support. My greatest thanks go to her.

TABLE OF CONTENTS

LIST OF TABLES

LIST OF FIGURES

CHAPTER 1

INTRODUCTION

Seismic hazard analyses require an estimate of earthquake ground motions from future events. These predictions are achieved through Ground Motion Prediction Equations (GMPEs), which include a prediction of the median and the standard deviation of ground motion parameters. The difference between observed and predicted ground motions is termed the ground motion residual. It is useful to normalize these residuals by the standard deviation of the GMPE:

$$\epsilon_{ij}(T) = \frac{ln\left[Sa_{ij}(T)_{observed}\right] - ln\left[Sa_{ij}(T)_{predicted}\right]}{\sigma_j} \quad (1)$$

where $Sa_{ij}(T)_{observed}$ are the observed spectral accelerations at an oscillator period T at recording station i for the event j; $Sa_{ij}(T)_{predicted}$ are the spectral accelerations predicted by a given GMPE for station i and the event j (using the appropriate metadata); σ_j are the standard deviations predicted by the given GMPE; and $\epsilon_{ij}(T)$ are the normalized residuals, also called "epsilon values". In other words, the $\epsilon_{ij}(T)$ values are the number of standard deviations of the difference between an observed *lnSa* (the natural logarithm of the observed *Sa*) and the predicted mean *lnSa*. The event dependency of the standard deviation is due to the magnitude-dependency of the standard deviation.

The normalized residual values are often used in seismic hazard analyses and subsequent analyses of structural response. Structural analysis of nonlinear structures requires time history analyses. The input time histories are typically associated with a specified spectral acceleration value at a single period; however, the selected ground motion must also be compatible with a certain target response spectra. The procedure by which a ground motion matching a target spectra is called ground motion selection. One of the methods which are used to provide the target response spectrum is the Conditional Mean Spectra (CMS) method, which was introduced by Baker (2011). The $\epsilon_{ij}(T)$ values, introduced in Equation 1 are used in the CMS method calculations to define the target response spectrum (Baker, 2011).

This paper explores the effects of site response on the correlation structure of ground motion residuals. The residuals, $\epsilon_{ij}(T)s$, are correlated for two periods T_i and T_j. The correlation coefficient varies between minus one and one, based on how strongly the predicted and actual normalized residuals are correlated; stronger correlations show higher correlation coefficients and are closer to one. A positive correlation implies the tendency of residuals at both periods is to be high or low at the same time. A

negative correlation implies that residual at one period tends to be higher while the residual at the other period tends to be lower. The matrix of the correlation coefficient of $\epsilon_{ij}(T)$ within all oscillator periods is called the correlation structure.

A subset of ground motion records obtained at rock stations of active shallow crustal earthquakes was selected from the Next Generation Attenuation (NGA) database (PEER, 2005). The subset was chosen such that it represents an unbiased set with respect to GMPEs developed as part of the NGA project. Two hypothetical soil sites were constructed for the current research: the first soil profile is a soft soil site from the San Francisco Bay area with the resonance frequency of about 1 Hz and the second soil profile is a hypothetical stiff soil site which is classified as site C by the Uniform Building Code with resonance frequency of about 5 Hz.

In order to explore the effects of site response on the correlation structure of ground motion residuals, one-dimensional site response analyses were conducted on the constructed soil sites using the selected rock input motions. The correlation structures of the normalized residuals over the ground surface are compared with those of the input motions and conclusions are drawn with respect to the effect of site response.

This thesis is presented in a manuscript format. The introduction (this chapter) presents a general introduction to the work. Chapter 2 presents a literature review on topics that are relevant to this thesis. Chapter 3 is a manuscript derived from this research that was prepared for presentation to the 10th National Conference on Earthquake Engineering. The manuscript is meant to be an independent text; hence some of the introduction and literature review is repeated. Finally, the conclusions are repeated and expanded on Chapter 4 (conclusions). Additional information relevant to the study that could not be fit within the length limitations of the manuscript is given in the Appendix A. This information is presented with the aim of clarifying and expanding the results discussed in Chapter 3.

CHAPTER 2

LITERATURE REVIEW

The objective of this literature review is to provide the reader with a general knowledge of the foundations upon which this work is grounded. The present study investigates the effects of site response on the correlation structure of ground motion residuals. Attenuation relationships or ground motion prediction equations (GMPE), which are used to predict the ground motions for bedrock, and site response analysis, which captures the influence of soil site on the bedrock ground motions, have a significant role in understanding this study and are discussed in detail in this literature review.

SITE RESPONSE ANALYSIS

The influence of local site conditions on the nature of the ground motions and the damage they may cause have been observed and studied for many years. The early work of seismologists studied site amplification shows that they used to assume linear soil behaviour and they rarely considered the soil non-linearity in their assessments of site conditions (Finn, 1991). Seed and Idriss (1969) were the first to consider soil non-linearity in their work. Their new assumption was based on observing earthquakes in Niigata and Alaska in 1964, and the 1967 Caracas earthquake (Rodriguez-Marek, 2000).

The site amplification provisions in design codes are based on analysis of recorded data at small amplitudes and site response analyses for larger amplitudes. Earlier code provisions were based on average spectral shapes for various soil conditions that were developed by Seed et al. (1976) based on a statistical study of more than 100 records from 21 earthquakes. These spectral shapes are shown in Figure 1; note that the spectral shapes are more dependent on the site condition at longer periods in comparison to shorter periods. This fact led to the use of simplified response spectra shapes by the Applied Technology Council (1978) and later, with some revisions, by the Uniform Building Code of 1988 (Rodriguez-Marek, 2000).

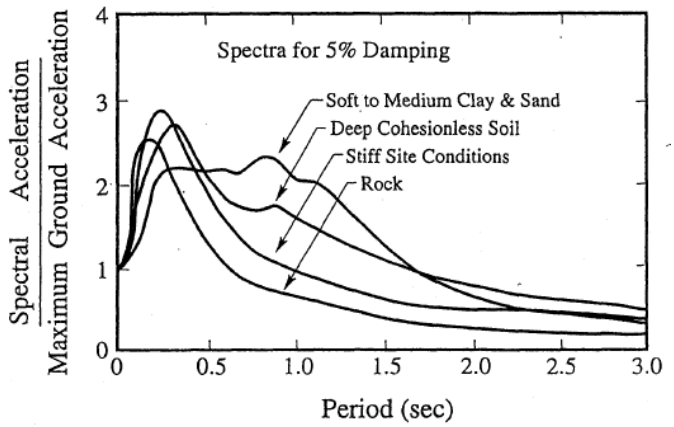

Figure1. Spectral shapes for different site conditions. "Ground motions and soil liquefaction during earthquakes." EERI Monograph Series, Earthquake Engineering Research Institute, Berkeley, CA. Used under fair use, 2013.

Ground response analysis is used to estimate the influence of site conditions on predicted response with respect to bedrock. Ground response analysis significantly affects the design response spectra and accordingly will influence the structural design. According to Kramer (1996) "Ground response analyses are used to evaluate dynamic stresses and strains for evaluation of liquefaction and to determine the earthquake- induced forces that can lead to instability of earth and earth-retaining structures."

Different site response analysis techniques have been developed over the years to solve for the influence of site over the motion applied at bedrock. These techniques are grouped based on the dimensionality of the problem. One-dimensional analysis assumes that the soil and rock surfaces are horizontal and also that the wave propagation is due to horizontal shear waves (SH) which move vertically through the bedrock. The linear approach is one of the methods used for one-dimensional site response analysis. The linear approach assumes that he soil behaves as a damped linear elastic material.

The ground response transfer functions (i.e. amplification factor), which are the key tools in ground response analysis, are used to compute various response parameters (i.e. ground surface acceleration) from an input motion parameter (i.e. as bedrock acceleration). In order to conduct one-dimensional response analysis, the Fourier transform of the input time history will be multiplied by the transfer function to produce the Fourier transform of the ground surface (output) motion. The last stage is to apply the inverse Fourier transforms to obtain the time history of the response parameter over the soil layer. Transfer functions determine how each frequency in the bedrock (input) motion is amplified or deamplified, by the soil deposit (Kramer, 1996).The transfer function is often chosen to be the ratio of ground motion at the soil surface to the ground motion over the bedrock and is called the Amplification Factor (AF). Amplification factors can be assessed for any ground motion parameters, but the response spectral acceleration is the most common parameter to use.

Bazzurro and Cornell (2004) studied the effect of the soil in terms of a site-specific and frequency-dependent amplification factor to identify the parameters that best predict AF for a generic frequency. They investigated Magnitude (*M*) and source-to-site distance (*R*) of input bedrock accelerogram along with bedrock ground motion parameters such as peak ground acceleration (PGA), the spectral acceleration values over the bedrock and the spectral acceleration values over ground surface at a generic frequency (f). The result showed the spectral acceleration is the most effective parameters to predict AF. They considered two case studies: a saturated sandy site and a saturated soft clay site.

EQUIVALENT LINEAR APPROACH

Methodologies to account for soil non-linearity were introduced in the 1960s and have been used since. In most engineering applications, the assumption of linear behaviour is insufficient. This is because neither the assumption nor the approach is realistic. The nonlinear approach, on the other hand, is complicated and cannot model the actual hysteretic stress-strain behaviour of cyclically loaded soil. Therefore, the equivalent linear method that modifies the linear approach may be an acceptable estimation of ground response for practical problems of interest (Kramer, 1996).

The equivalent linear model provides few parameters that represent typical soil behaviour when subjected to cyclic loading. This model is based on a hysteresis loop which is shown in Figure 2. This loop has two important shape characteristics: inclination of the loop that depends on the stiffness of the soil and can be quantified by the secant stiffness ($Gsec$), and the breadth which represents the energy dissipation (W_D). The Damping Ratio (ξ) is a measure of energy dissipation and is given by:

$$\xi = \frac{W_D}{4\pi W_S} = \frac{1}{2\pi} \frac{A_{loop}}{G_{sec}\,\gamma_c^2} \qquad (2)$$

where W_D is the dissipated energy, W_S the maximum strain energy, γ_c the shear strain, and A_{loop} the area of the hysteresis loop as is shown in Figure 2.

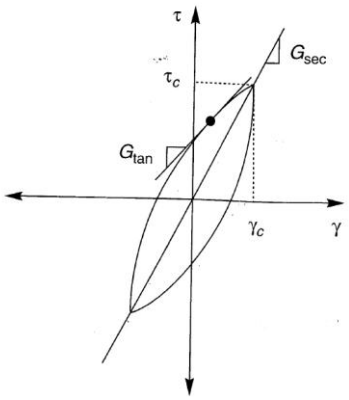

Figure 2. secant shear modulus, Gsec and tangent shear modulus, Gtan. Kramer, S. L. (1996). Geotechnical Earthquake Engineering. Upper Saddle River, NJ: Prentice-Hall, Inc. Used under fair use, 2013.

The parameters G_{sec} and ξ are often referred to as equivalent linear material parameters, which are different for each site and each soil layer. Laboratory tests show that G_{sec}, which is the general inclination of the hysteresis loop is a factor of cyclic shear strain amplitude. The equivalent linear approach uses these parameters, assuming G_{sec} and ξ are constants for each soil layer for a given strain level. At this method, the shear strain is computed for each layer and the new constant parameters needed to be calculated for each layers such that the new parameters are compatible with each layer's new shear strain (see Figure 3). In the equivalent linear method, an iteration procedure is used to make sure the parameters used in the analysis are compatible with the computed strain level in all the layers (Kramer, 1996)

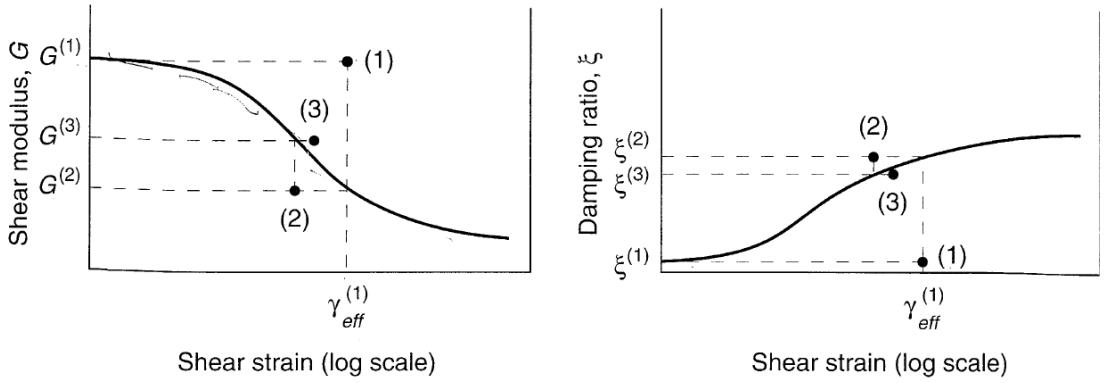

Figure 3. Equivalent linear approach process. Kramer, S. L. (1996). Geotechnical Earthquake Engineering. Upper Saddle River, NJ: Prentice-Hall, Inc. Used under fair use, 2013.

The computer program Strata is used in the current research as the site response analysis software. This software uses the equivalent linear approach in the frequency domain. Strata uses one-dimensional site response analysis which applies linear wave propagation with strain dependent dynamic soil properties. The equivalent linear analysis method was first used in the computer program SHAKE

(Schnabel et. al.,1972; Idriss and Sun, 1992). According to Kottke and Rathje (2008), both SHAKE and Strata only compute the response for vertically propagating, horizontally polarized shear waves propagated through a site with horizontal layers.

GROUND MOTION PREDICTION EQUATION (GMPE)

Ideally, the ground response analyses are used to model the rupture mechanism at the source of an earthquake and the seismic wave propagation through the earth to the top of the bedrock and at ground surface. However, the rupture mechanism and the wave propagation processes are highly complicated and as a result ground response analysis is not commonly applied in the engineering field. In practice, Ground Motion Prediction Equations (GMPEs) are used to predict the ground motions over the bedrock along with site response analysis which is applied to consider the effect of site on the bedrock ground motions (Kramer, 1996). However, most GMPEs include in the set of predictor variables for the site specific shear wave velocity can be used to compute the ground motions at the ground surface directly.

Ground-motion prediction equations provide ground-motion intensity measures such as peak ground motions or response spectra as a function of earthquake magnitude and distance and in some cases, other variables. These measurements are important tools in the analysis of seismic hazard. These equations are mostly derived by applying statistical methods, especially regression methods of recorded strong motion databases. The amount of data used in regression analysis to develop GMPEs plays a crucial role in the degree of reliability of the resulting attenuation relationships especially in magnitude and distance ranges that are important for seismic hazard analysis. (Boore and Atkinson, 2008).

In the current research three different NGA ground motion prediction equations are used to predict the ground motions over the bedrock: Abrahamson and Silva (2008), known as AS08, Boore and Atkinson (2008), known as BA08, and Chiou and Young (2008), known as CY08. These GMPEs were derived using empirical regression of an extensive strong-motion database compiled by the Pacific Earthquake Engineering Research Center's Next Generation Attenuation (PEER NGA) project. The GMPE equations used an extensive database of thousands of records, compiled from shallow crustal earthquakes in active tectonic environments worldwide.

The BA08 GMPE model is for average horizontal component ground motions and is expressed as a function of earthquake magnitude, distance from source to site, local average shear-wave velocity, and fault type. The predicted attenuation parameters are peak ground acceleration (*PGA*), peak ground velocity (*PGV*), and 5%-damped pseudo-absolute-acceleration spectra (*PSA*) at periods between 0.01 s and 10 s. The BA08 model used 14 times more data, as compared to GMPEs that were published by

Boore and his colleagues in 1997, to derive the equation. The increase in data quantity is more critical for *PSA.* The database used for this model is PEER-NGA empirical strong-motion database (Boore and Atkinson 2008).

The CY08 model is another GMPE applied for estimating horizontal ground motion amplitudes caused by shallow crustal earthquakes occurring in active tectonic environments. The attenuation parameters provided by the CY08 model are peak acceleration, peak velocity, and 5%-damped *PSA* for spectral periods of 0.01 to 10 seconds. The database used for this model is PEER-NGA empirical strong-motion database (Chiou et al., 2008).

The AS08 model is an empirical ground-motion model for the rotation independent average horizontal component from shallow crustal earthquakes and is derived using the PEER NGA database. AS08 is applicable to the distances between 0 to 200 km, the periods of 0 to 10 s and the average to large earthquakes with magnitudes of 5 to 8.5 (Abrahamson and Silva, 2008).

The NGA models mentioned above are globally applicable to shallow crustal earthquakes in active regions, and can be used for both soil and rock sites; however, they differ in some features. One of the differences within these models is consideration of aftershocks in the data set used to derive the equations. The AS08 and CY08 data sets include aftershocks, resulting in a much larger number of earthquakes than the BA08 sets. The BA08 model has the simplest parameterization within the introduced models. The BA08 model includes magnitude, distance and the style of faulting which are common for all models. However, AS08 and CY08 models, on the other hand, include additional parameters for hanging wall (HW) effects, rupture-depth effects, and soil sediment depth effects which make them more complicated.

Distance, besides the earthquake magnitude, is one of the most important parameters and has a significant influence on prediction of spectral acceleration. Different types of distances are introduced by the NGA dataset. The distance used at BA08 is R_{JB} which is the closest horizontal distance to the surface projection of the rupture plane. The AS08 and CY08 models use R_{rup} which is the closest distance to the rupture plane. Also, R_x which is a distance term is used by the AS08 and CY08 models for incorporating hanging wall (HW) effects. Rx is defined as the horizontal distance from the top edge of the rupture, measured perpendicularly to the fault strike. R_x is positive over the hanging wall and negative over the footwall (Abrahamson et al., 2008). Figure 4, demonstrates different types of distance measures used in the NGA Ground motion prediction equations.

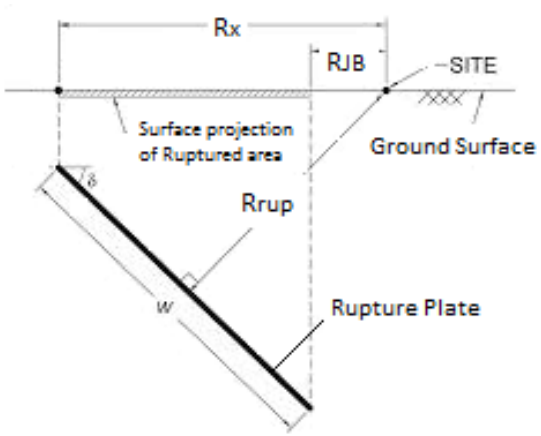

Figure 4. Demonstration of R_x, R_{JB} and R_{rup} distances.

One of the most important differences within NGA models used in the current research is the difference in the forms of the standard deviation models applied to compute the standard deviation of a predicted response parameter for a given period. The AS08 and CY08 models have magnitude-dependent standard deviation models and the BA08 model has magnitude-independent standard deviations. Also, AS08 and CY08 models include the nonlinear site amplification effects on standard deviation, whereas BA08 model does not. (Abrahamson et al., 2008). Some of the main features of the aforementioned NGA models are summarized in Table 1 below.

Table 1. Main features of NGA models. Abrahamson, N., and Silva, W. (2008). " Summary of the Abrahamson & Silva NGA ground motion Relations", Earthquake Spectra 24 , 67–97. Used under fair use, 2013.

	AS08	BA08	CB08	CY08	I08
Saturation at short distances	X	X	X	X	X
Style-of-faulting factor	X	X	X	X	X
Rupture depth factor	X	Implicit through R_{JB}	X (RV only)	X	
HW factor	X	Implicit through R_{JB}	X	X	
Nonlinear site amplification	Constrained (Walling et al., 2008)	Constrained (Choi & Stewart, 2005)	Constrained (Walling et al., 2008)	X	N/A
Soil/sediment depth factor	Constrained (Shallow: Silva, 2005; deep: Day et al., 2005)		Constrained deep: Day et al. (2005)	X	N/A
Magnitude dependent σ	X			X	X
Nonlinear effects on σ	Intra-event and intra-event terms		Intra-event term only	Intra-event and intra-event	

The AS08 and CY08 models. which include magnitude dependent standard deviation, also include aftershocks, which lead to an increase in the number of small magnitude earthquakes and more variability in comparison to the BA08 model which includes just large magnitude earthquakes. Also, the AS08 and CY08 models include the nonlinear effects on site amplification, but BA08 does not. Figures 5-7 show the standard deviation dependence on period, magnitude and distance.

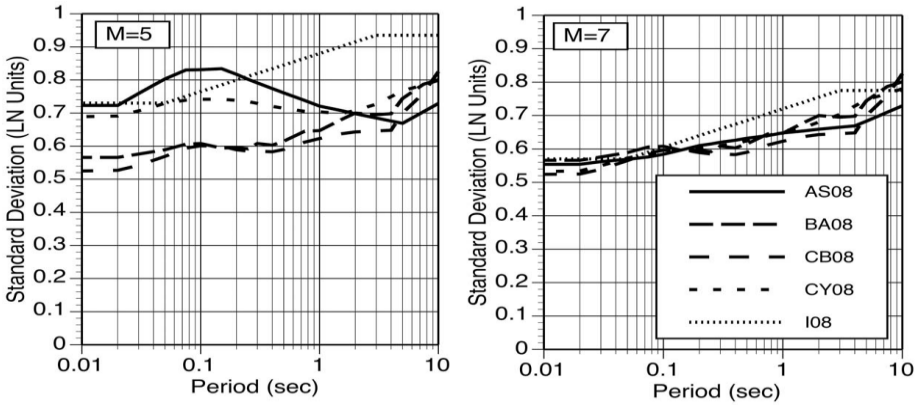

Figure 5. Comparison of the standard deviation for M5 (left) and M7 (right) strike-slip earthquakes at a distance of 30 km for rock site conditions (VS30=760 m/ s). Abrahamson, N., and Silva, W. (2008). " Summary of the Abrahamson & Silva NGA ground motion Relations", Earthquake Spectra 24 , 67–97. Used under fair use, 2013.

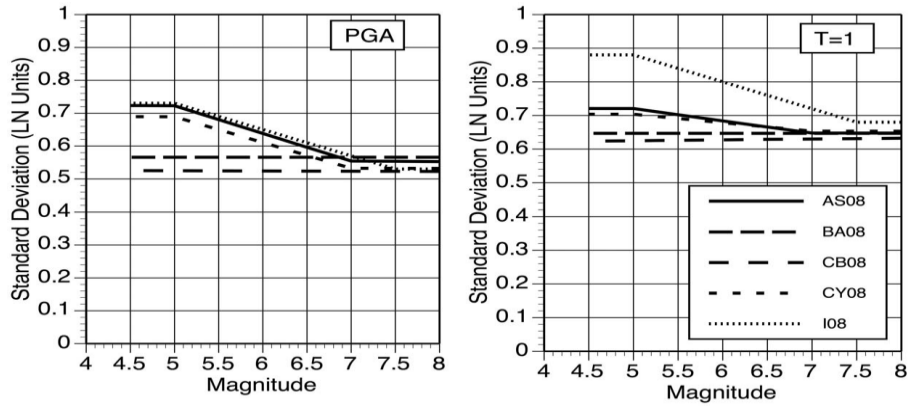

Figure 6. Comparison of magnitude dependence of the standard deviation for *PGA* (left) and T=1 sec (right) for strike-slip earthquakes at a distance of 30 km for rock site conditions (V_{S30}=760 m/ s). Abrahamson, N., and Silva, W. (2008). " Summary of the Abrahamson & Silva NGA ground motion Relations", Earthquake Spectra 24 , 67–97. Used under fair use, 2013.

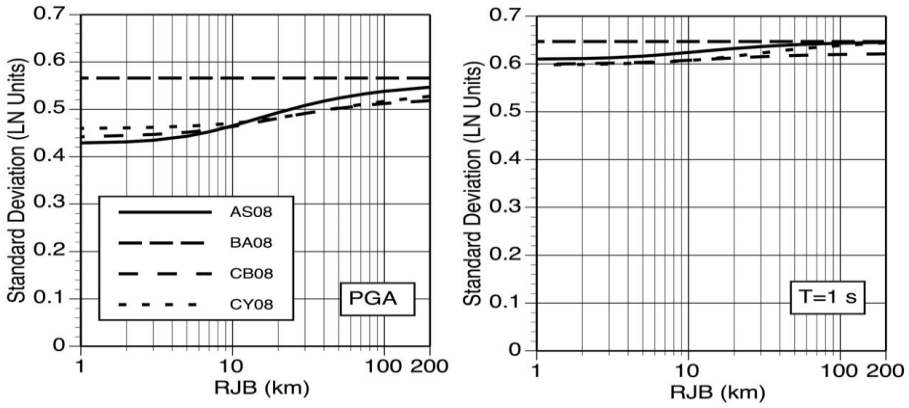

Figure 7. Comparison of distance dependence of the standard deviation for *PGA* (left) and spectral acceleration at T=1 sec. (right) for M7 strike-slip earthquakes and soil site conditions (V_{S30}=760 m/ s). Abrahamson, N., and Silva, W. (2008). " Summary of the Abrahamson & Silva NGA ground motion Relations", Earthquake Spectra 24 , 67–97. Used under fair use, 2013.

CORRELATION COEFFICIENT FOR SPECTRAL ACCELERATION RESIDUALS

Seismic hazard analyses require an estimate of earthquake ground motions from future events. The differences between observed and predicted ground motions, when normalized by the standard deviation, are referred to as epsilon (ϵ). Baker and Cornell (2006) observed that the residuals of horizontal ground motions at different oscillator periods are correlated. For spectral accelerations, the correlation structure of normalized residuals across oscillator periods is important for guiding ground motion selection.

Correlation structures of $\epsilon(T)$ for a large global dataset have been studied extensively. These correlation structures reflect effects that are averaged over the entire datasets underlying the analyses. Baker and Jayaram (2008) computed the correlation structure for the Next Generation Attenuation (NGA) ground motion database using the entire set of GMPEs developed as part of the NGA project (Power et. al. 2008). The correlation models proposed by Baker and Jayaram (2008) are independent of site condition, hence they assume that the effect of site amplification is captured by the median predictions and are not observed in the correlation of ground motion residuals. The correlation structure of residuals between two sets of periods, developed by Baker and Jayaram (2008), is shown in Figure 8.

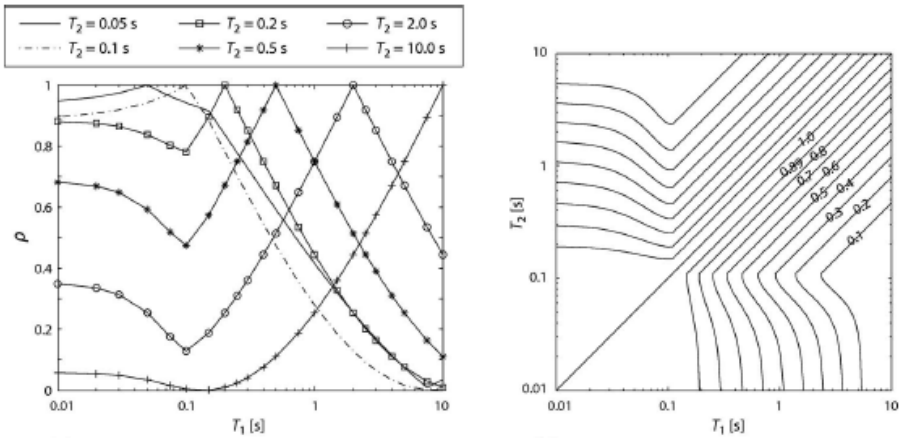

Figure 8. (a) Plots of correlation coefficients versus T1 , for several T2 values (b) Contours of correlation coefficients versus T1 and T2. Baker, J. and Jayaram, N. (2008). "Correlation of Spectral Acceleration Values from NGA Ground Motion Models." Earthquake Spectra 24(1), 299-317. Used under fair use, 2013.

Many other investigations have been conducted to find the correlation of other intensity measures (IMs). For instance, Bradley (2011) investigated the correlation between peak ground velocity (*PGV*) and spectrum intensity measured (for 5% damped spectral acceleration). The results indicate that *PGV* is strongly correlated with spectrum intensity (*SI*), moderately correlated with medium to long-period pseudo spectral acceleration (*SA)* and also moderately correlated with short period spectral acceleration, *PGA* and acceleration spectrum intensity (*ASI*).

CHAPTER 3

EFFECTS OF SITE RESPONSE ON THE CORRELATION STRUCTURE OF GROUND MOTION RESIDUALS

ABSTRACT

Seismic hazard analyses require an estimate of earthquake ground motions from future events. These predictions are achieved through Ground Motion Prediction Equations, which include a prediction of the median and the standard deviation of ground motion parameters. The differences between observed and predicted ground motions, when normalized by the standard deviation, are referred to as epsilon (ϵ). For spectral accelerations, the correlation structure of normalized residuals across oscillator periods is important for guiding ground motion selection. Correlation structures of $\epsilon(T)$ for a large global dataset have been studied extensively. These correlation structures reflect effects that are averaged over the entire dataset underlying the analyses. This paper considers the effects of site response on the correlation structure of normalized residuals. This is achieved by performing site response analysis for two hypothetical soil profiles using a set of 85 rock input motions. Results show that there is no significant difference between the correlation structure for rock ground motions and the correlation structure after considering the influence of site response analysis.

INTRODUCTION

Seismic hazard analyses require an estimate of earthquake ground motions from future events. These predictions are achieved through Ground Motion Prediction Equations (GMPEs), which include a prediction of the median and the standard deviation of ground motion parameters. The difference between observed and predicted ground motions is termed ground motion residual; when the residuals are normalized by the standard deviation of the GMPE, the resulting equation is:

$$\epsilon_{ij}(T) = \frac{ln\left[Sa_{ij}(T)_{observed}\right] - ln\left[Sa_{ij}(T)_{predicted}\right]}{\sigma_j} \quad (1)$$

where $Sa_{ij}(T)_{observed}$ are the observed spectral accelerations at an oscillator period T at recording station i for the event j; $Sa_{ij}(T)_{predicted}$ are the spectral accelerations predicted by a given GMPE for station i and the event j (using the appropriate metadata); σ_j are the standard deviations predicted by the given GMPE; and $\epsilon_{ij}(T)$ are the normalized residuals, also called "epsilon values". In other words, the $\epsilon_{ij}(T)$ values are

the number of standard deviations of the difference between an observed *lnSa* (the natural logarithm of the observed *Sa*) and the predicted mean *lnSa*. The event dependency of the standard deviation is due to the magnitude-dependency of the standard deviation.

The normalized residual values are often used in seismic hazard analyses and subsequent analyses of structural response. Structural analysis of nonlinear structures requires time history analyses. The input time histories are typically associated with a specified spectral acceleration value at a single period; however, the selected ground motion must also be compatible with a certain target response spectra. The procedure by which a ground motion matching a target spectra is called ground motion selection. One of the methods which are used to provide the target response spectrum is the Conditional Mean Spectra (CMS) method, which was introduced by Baker (2011). The $\epsilon_{ij}(T)$ values, introduced in Equation 1 are used in the CMS method calculations to define the target response spectrum (Baker, 2011).

This paper explores the effects of site response on the correlation structure of ground motion residuals. The residuals, $\epsilon_{ij}(T)$, are correlated for two periods T_k and T_l. The correlation coefficient varies between negative one and one depending on the type of correlation between the predicted and actual normalized residuals. The matrix of the correlation coefficient of $\epsilon_{ij}(T)s$ within all oscillator periods is called the correlation structure.

A subset of ground motion records from active shallow crustal earthquakes obtained at rock stations was selected from the NGA database (PEER, 2005). The subset was chosen such that it represents an unbiased set with respect to GMPEs developed as part of the Next Generation Attenuation Relationships (NGA) project. Two hypothetical soil sites were constructed for the current research: the first soil profile is a soft soil site from the San Francisco Bay are with high resonance frequency of about 1 Hz. The second soil profile is a hypothetical stiff soil site which is classified as site C by the Uniform Building Code with resonance frequency of about 5 Hz.

In this paper, after a brief review of similar studies in this field, the ground motion data used in this study is described, along with a description of the sites used for the site response analyses. The methodology section contains the computed correlation structure of residuals for bedrock and soil sites after conducting site response analysis and explores the effects of site response on the correlation structure of ground motion residuals. Finally, some of the important results of this study are highlighted in the conclusion.

BACKGROUND

The correlation structure of normalized residuals for spectral acceleration across oscillator periods is important for guiding ground motion selection. Correlation structures of $\epsilon_{ij}(T)$ for a large global dataset have been studied extensively. These correlation structures reflect effects that are averaged over the entire datasets underlying the analyses.

Baker and Cornell (2006) observed that the residuals of horizontal ground motions at different oscillator periods are correlated. Later, Baker and Jayaram (2008) computed the correlation structure for the Next Generation Attenuation (NGA) ground motion database using the entire set of GMPEs developed as part of the NGA project (Power et. al. 2008). The correlation models proposed by Baker and Jayaram (2008) are independent of site condition, hence they assume that the effect of site amplification is captured by the median predictions and are not observed in the correlation of ground motion residuals. The correlation structure of residuals between two sets of periods, developed by Baker and Jayaram (2008), is shown in Figure 9.

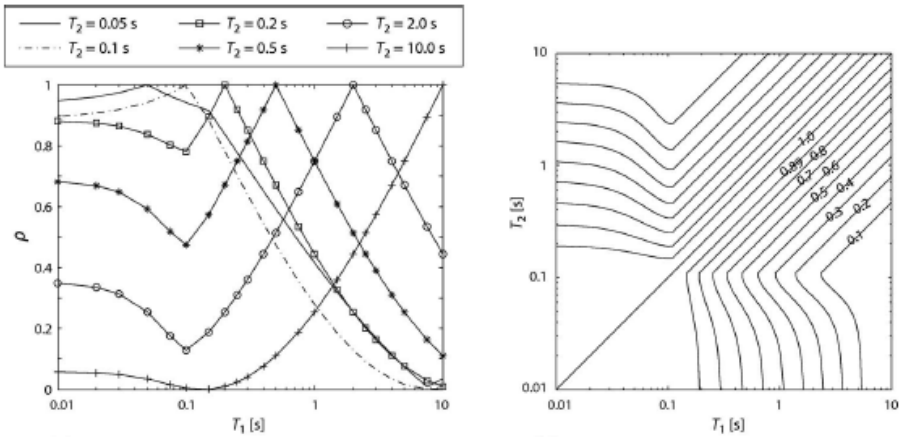

Figure 9. (a) Plots of correlation coefficients versus T1 , for several T2 values (b) Contours of correlation coefficients versus T1 and T2. Baker, J. and Jayaram, N. (2008). "Correlation of Spectral Acceleration Values from NGA Ground Motion Models." Earthquake Spectra 24(1), 299-317. Used under fair use, 2013.

STRONG GROUND MOTION DATA BASE

In order to explore the effects of site response on the correlation structure of ground motion residuals, we first created a database of a set of ground motions recorded on bedrock from the Next Generation Attenuation (NGA) ground motion database. This set was used as input motions for site response analyses. The ground motions were chosen such that they represent an unbiased set with respect to GMPEs developed as part of the NGA project. Selection criteria were established as follows:

$6.3 < Mw < 7.9$

500 m/s < V_{s30} < 1600 m/s

20 km < R_{Jb} < 150 km

The intent of this selection was such that the V_{s30} was high enough so that all the records corresponded to true rock stations. The original target for a minimum V_{s30} was 760 m/s (i.e., the B-C boundary in the site classifications in the Uniform Building Code); however, a sufficient amount of records were not found that satisfied that criteria, hence the minimum V_{s30} was reduced to 500 m/s. Distances were kept to larger than 20 km to avoid records with strong near-field effects and to less than 150 km to avoid records that were dominated by surface waves. A total of 85 ground motions were selected such that the above criteria were satisfied. These records come from 14 different earthquakes at both horizontal directions that occurred worldwide (see Table 3A in the appendix A).

Most of the selected records are from four earthquakes: 17 January 1994 Northridge earthquake, 18 October 1989 Loma Prieta earthquake, 20 September 1999 Chi-Chi, Taiwan earthquake and 25 September 1999 Chi- Chi, Taiwan earthquake. The last earthquake is an aftershock of the 20 September earthquake. However, according to Bazzurro and Cornell (2004), the concentration of the recordings does not statistically affect the result. The metadata for all 85 selected ground motions are presented in Table 2A in the appendix A.

DESCRIPTION OF SITE PROFILES

Two different soil sites were chosen for the current research. The first is a soft soil site, which is a typical Bay Mud site from the San Francisco Bay region. The second profile is a very stiff soil site, which is classified as site C by the Uniform Building Code (i.e.360 m/s < $Vs \leq$ 760 m/s). The following sections describe each site in detail.

SOFT SOIL SITE

A hypothetical soft-soil site with a strong resonance period of about 1 s was constructed and one-dimensional site response analysis was conducted for the 85 selected ground motions from active shallow crustal earthquakes. The soil site is a typical Bay Mud site from the San Francisco Bay region (Rodriguez-Marek and Bray, 2006).

Soil sites with relatively low resonance frequencies can result in high damages during earthquakes. According to Kalkan et al. (2008), who conducted a study in this regard in the Bay area, the site

amplification increases the seismic shaking potential by more than a factor of 2 in areas underlain by bay mud and by factors of more than 1.5 in areas underlain by Holocene alluvium. The site shear wave velocity and density profiles for the soft soil site are shown in Figure 10.

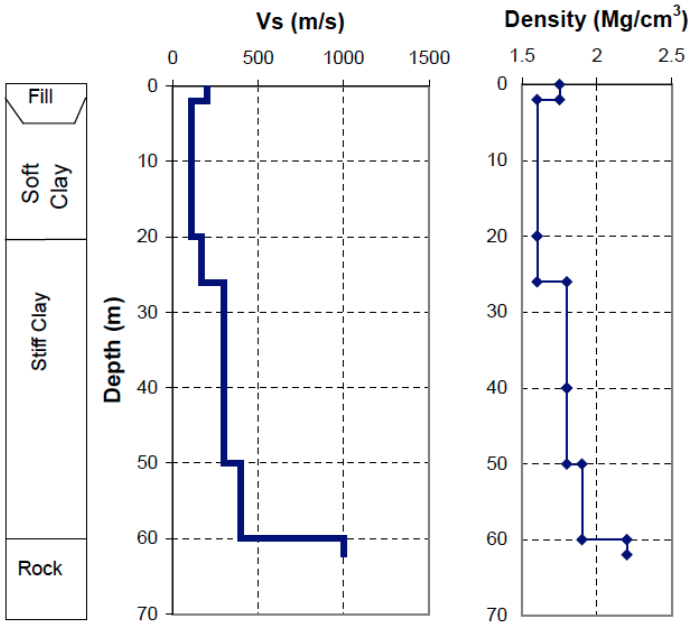

Figure 10. Generic Soft Clay shear wave velocity and density profiles. The profile represents typical Bay Mud sites from the San Francisco Bay region. Rodriguez- Marek, A. (2000). "Near-Fault Seismic Site Response" University of California, Berkeley, ProQuest, UMI Dissertations Publishing, 2000. 3002238. Used under fair use, 2013.

Site response analyses were conducted using the equivalent linear method through the software Strata (Kottke and Rathje, 2008). The Isenhower and Stokoe model (1981) was used as the modulus of reduction and damping curves for soft clay along with the Vucetic and Dobry (PI=30) model (1991) being for the stiff clay. The curves for the models are shown in Figures 11 and 12, respectively.

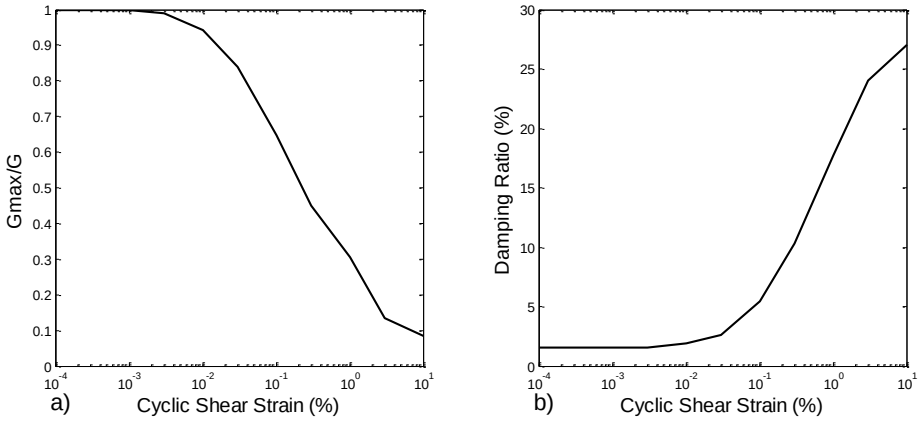

Figure 11. The Isenhower and Stokoe (1981) modulus of reduction and damping curves used for soft clay.

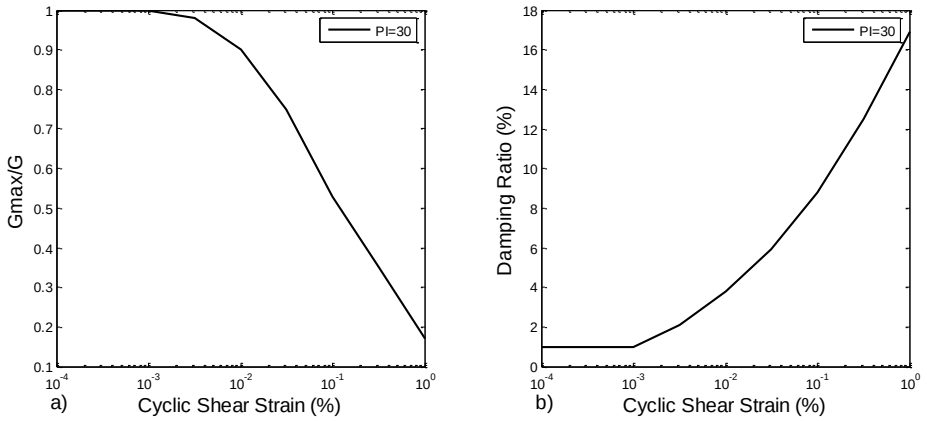

Figure 12. The Vucetic and Dobry (PI=30) model (1991) modulus of reduction and damping curves used for stiff clay.

Some assumptions which were made in the site response analyses are as follows: the unit weight of rock was assumed to be 2243 kg/m^3 (140 pcf) and the damping ratio of rock was equal to 1%. The maximum number of iterations was 20 and the error tolerance was 2%. The effective strain ratio was 0.65 and the maximum frequency was set to be 25 Hz. The soil profile was divided into 85 layers in order to perform the site response analysis with Strata. The thickness of the first 54 layers was 0.5 m and the thickness of the rest of the layers was set to 1 m.

Figure 13 shows the depth versus peak shear strain and the depth versus peak ground acceleration (*PGA*) computed using the 1020 record measured during the 17 January 1994 Northridge earthquake. As is shown, the shear strain and *PGA* decrease with depth. The shear strain and *PGA* values increase at the depth of 20 m, which is the beginning of the soft clay layer. The shear strain values shown in Figure 13a, fall below failure level through the profile (failure level of 1%) which meets the site response analysis assumption in this regard.

Figure 14 depicts spectral acceleration versus period over both bedrock and ground surface of the same earthquake for periods between 0.01s to 10s. The spectral accelerations over the ground surface are higher at most of the periods which shows the amplification in soil site. However, the spectral accelerations at rock are higher between 0.06s to 0.1s, which implies deamplification for those periods.

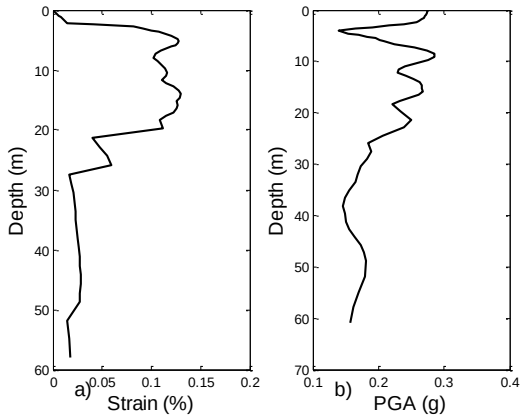

Figure 13. a) Peak shear- strain profile (b) Peak ground acceleration profile for the 1020 record measured during the 17 January 1994 Northridge earthquake.

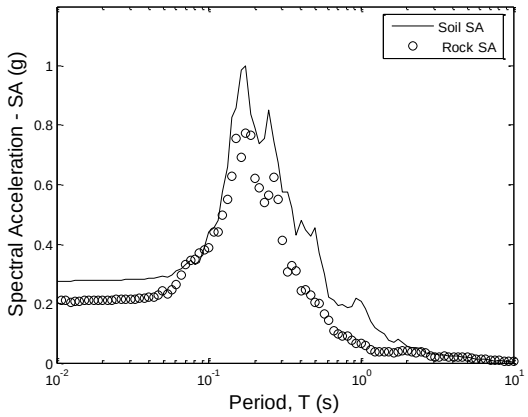

Figure 14. a) Spectral acceleration over the bedrock and ground surface regarding the 1020 record measured during the 17 January 1994 Northridge earthquake.

VERY STIFF SOIL SITE

A hypothetical stiff-soil site which is classified as site C by the Uniform Building Code (i.e. 360 m/s < *Vs* ≤ 760 m/s) was constructed and one-dimensional site response analyses were conducted for the 85 selected ground motions from active shallow crustal earthquakes. The site shear wave velocity profile is shown in Figure 15 (Rodriguez-Marek, 2000).

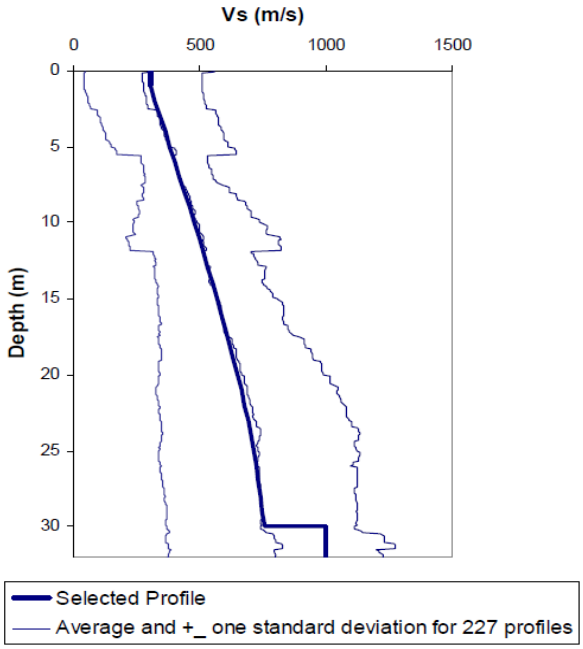

Figure 15. Selected shear wave velocity profile for the Very Stiff Soil profile (Site C).Included in the graph are the median and ± one standard deviation for a database including 227 profiles. classified as Site C by the Uniform Building Code (Rodriguez-Marek 2000 - used under fair use, 2013).

The equivalent linear method was also used as a site response analysis approach for the very stiff soil profile. The Idriss (1990) model regarding sand is used for both modulus of reduction and damping curves. The curves for this model are shown in Figure 16 below:

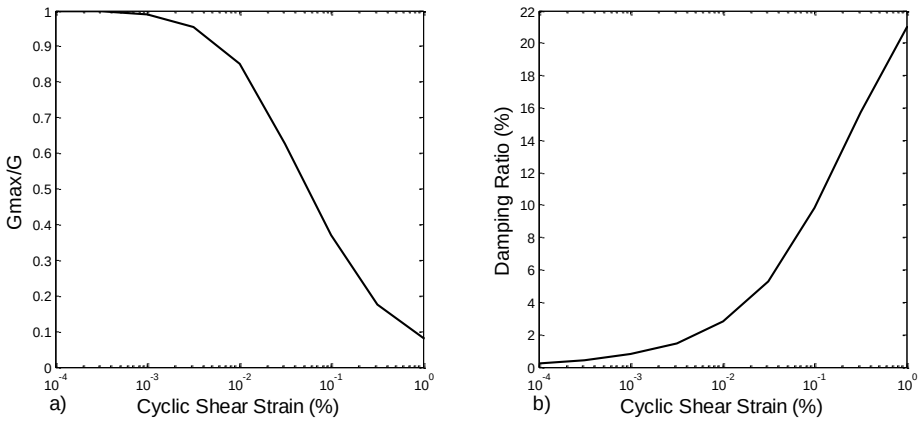

Figure 16. The Idriss (1990) model modulus of reduction and damping curves used for very stiff soil (sand).

The site response analysis for the stiff soil profile is mostly based on the same assumptions as the soft soil profile. These assumptions are as follows: the unit weight of rock was assumed to be 2243 kg/m^3 and the damping ratio of rock was equal to 1%. The maximum number of iterations was 20 and the error tolerance was 2%. The effective strain ratio was 0.65 and the maximum frequency was set to be 25 Hz. The soil profile was divided into 67 layers in order to perform the site response analysis with Strata.

Figure 17 shows the depth versus peak shear strain and the depth versus peak ground acceleration (*PGA*) plots at the ground surface for the same plots of the same ground motion at the soft soil profile. The shear strain profile for the stiff soil site falls below the failure level (1%) for stiff soil site, the same as soft soil profile, which seems reasonable. As is shown, the shear strain and *PGA* plots follow the same pattern as the soft soil profile. The strain values increase in the top 20 m of the stiff soil which has V_s values less than 500 m/s and represents softer portion of second soil profile. However, as shown in Figure 14 b, the *PGA* profile plot is more uniform in comparison to the same plot for soft soil (Figure 13b). As can be seen, the PGA shift from bedrock to soil profile is more significant for very stiff soil in comparison to soft soil. This conclusion is also derived by Sykora et al. (1996) in a related study. Figure 18 depicts spectral acceleration versus period over both bedrock and ground surface of the 1020 record measured during the 17 January 1994 Northridge earthquake, for periods between 0.01s to 10s. For stiff soil site and this specific ground motion, the soil spectral acceleration values are higher than rock spectral acceleration values. This implies the amplification and can be seen through all periods.

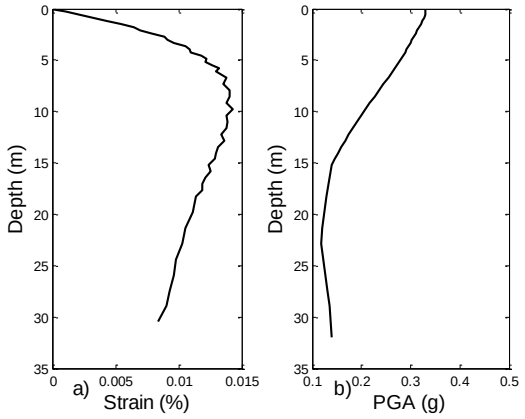

Figure 17. a) Max shear- strain profile (b) Peak ground acceleration profile for the 1020 record measured during the 17 January 1994 Northridge earthquake.

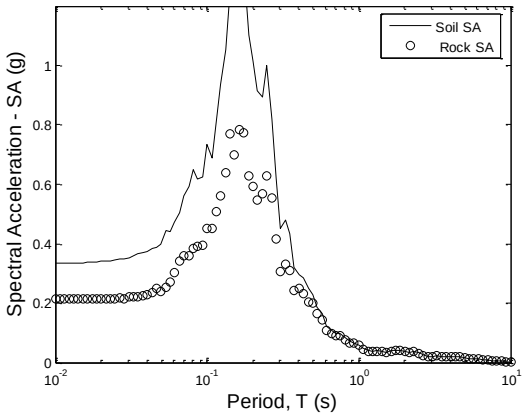

Figure 18. a) Spectral acceleration over the bedrock and ground surface regarding the 1020 record measured during the 17 January 1994 Northridge earthquake.

METHODOLOGY

In this paper, the effect of site response on the correlation structure of ground motion residuals is explored. This influence is investigated by computing the correlation structure of normalized residuals, $\epsilon_{ij}(T)$, over both bedrock and ground surface. The correlation structure of $\epsilon_{ij}(T)$ over bedrock was explored before by Baker and Jayaram (2008) over a different data set. The result of this research is presented in this paper for comparison. In order to investigate the correlation structure of $\epsilon_{ij}(T)$ over ground surface, site response analysis is conducted using 85 worldwide bedrock input motions from active shallow crustal earthquakes.

CORRELATION STRUCTURE of $\epsilon_{ij}(T)$ OVER BEDROCK

The $\epsilon\ (T)$ values over bedrock are obtained using Equation 1.For each record and period, the predicted and observed spectral acceleration values were calculated and used in Equation 1 to compute $\epsilon_{ij}(T)$values. This computation is performed for 85 ground motions to see how their $\epsilon_{ij}(T)$ values statistically relate to each other at periods varied between 0.01s to 10s. "Observed" spectral acceleration in this research refers to the geometric mean of two orthogonal horizontal spectral acceleration components of ground motions at each period. Figure 19 shows the spectral acceleration plots of the 85 selected ground motions. The red lines show the mean and the standard deviation of spectral acceleration values. The "predicted" spectral acceleration, $Sa_{ij}(T)_{predicted}$, values for the 85 ground motions are calculated using three NGA ground motion models (GMPEs): Abrahamson and Silva (2008), Boore and Atkinson (2008) and Chiou and Young (2008). In this paper, the results of applying the Abrahamson and Silva (2008) model are presented.

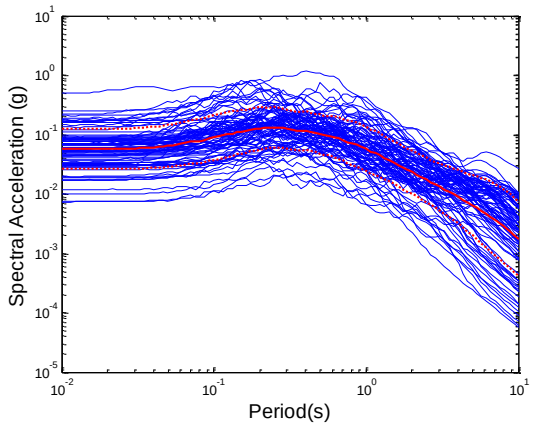

Figure 19. Spectral Acceleration over bedrock for the 85 selected ground motion records. The solid red line is the mean of all records, and the dotted red lines are the mean plus/minus one standard deviation.

The normalized residuals at the bedrock were computed applying the observed and the predicted spectral accelerations in Equation 1. Figure 20 shows the scatter plot of $\epsilon_{ij}(T)$ values versus 85 ground motions for two individual periods of 0.1s and 1s which includes the mean and the mean plus/minus one standard deviation as well (the black lines). Also, Figure 21 shows the mean and the standard deviation variation at each period for all ground motions. Although the mean and the standard deviations oscillate around their predicted values of zero and one, respectively, there is a slight bias away from these values that can be seen at some periods (Figure 21).

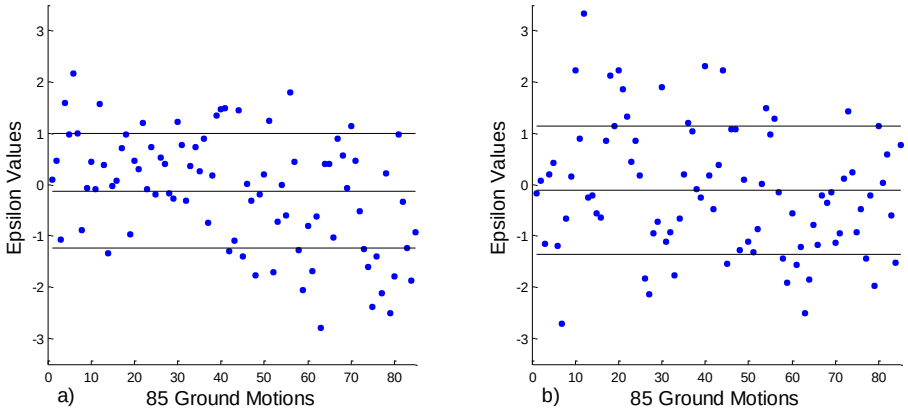

Figure 20. Scatter plot of $\epsilon_{ij}(T)$ for the 85 ground motions regarding the periods of a) T= 0.1s, and b) T= 1s. The black lines represent the mean and the mean plus/minus one standard deviation.

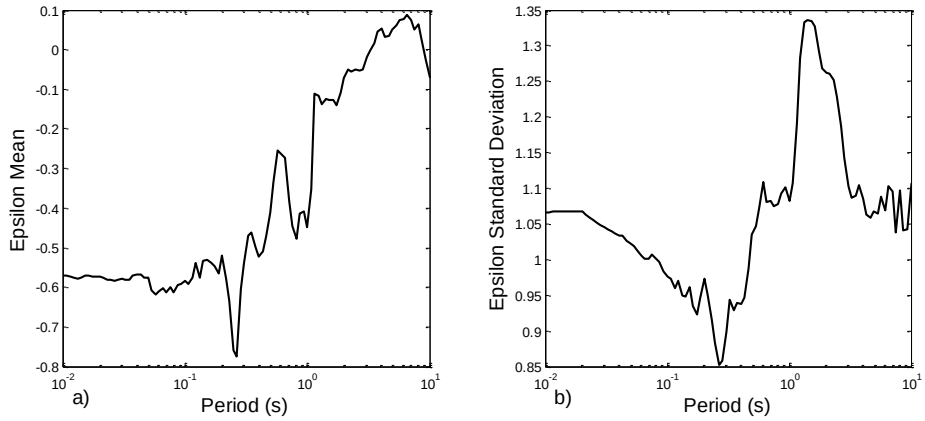

Figure 21. The mean and standard deviation of $\epsilon_{ij}(T)$ values versus periods between 0.1s to 10s for bedrock.

Figure 22a presents the correlation structure of $\epsilon_{ij}(T)$values for a selected set of periods, T_2, and a range of periods between 0.01 and 10 seconds, T_1, for bedrock. Observe that this correlation structure is similar to the correlation structure of $\epsilon_{ij}(T)$ obtained by Baker and Jayaram (2008) (see Figure 9). Figure 22b shows the same result using contour lines to illustrate the correlation structure of $\epsilon_{ij}(T)$ values over the entire period range.

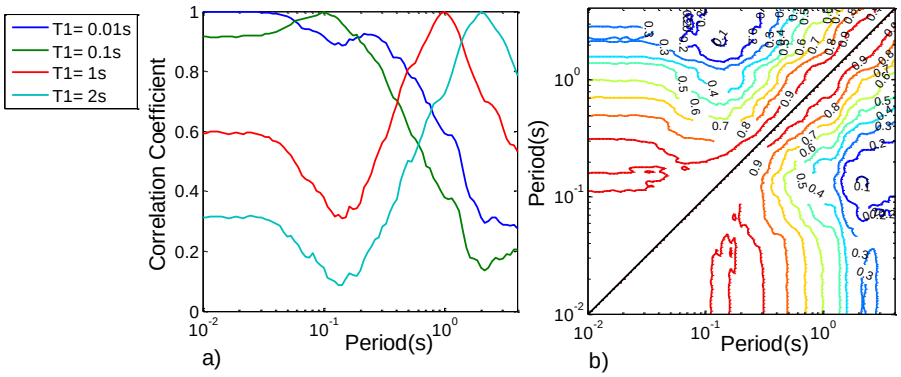

Figure 22. Correlation coefficients for bedrock obtained using AS08. Correlation coefficients for (a) Selected periods (T1), and (b) entire period range.

CORRELATION STRUCTURE of $\epsilon_{ij}(T)$ VALUES ACCOUNTING FOR THE EFFECTS OF SITE RESPONSE

In order to develop the correlation structure of residuals, including the effects of site response, two hypothetical soil sites, as described in Figures 10 and 15, were constructed. One-dimensional site response analyses were conducted for the selected ground motions using Strata. The normalized residuals at the ground surface were computed using Equation 1, but the ground motions predicted by site response were used as "observed" ground motions in-lieu of recorded ground motions. The correlation structure of

the normalized residuals over the hypothetical soil profiles shows the effect of site response on the correlation structure obtained for bedrock. The spectral acceleration mean values, shown as solid red line in Figures 23 and 19, are slightly higher after the influence of site response analysis that shows the soil amplification.

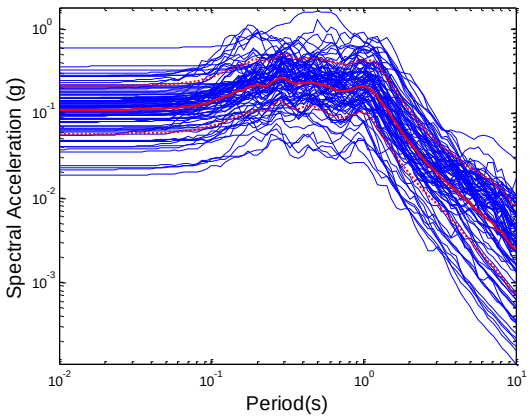

Figure 23. Spectral Acceleration over soft soil site for the 85 selected ground motion records. The solid red line is the mean of all records, and the dotted red lines are the mean plus/minus one standard deviation.

The predicted spectral accelerations, $Sa_{ij}(T)_{predicted}$, for the 85 ground motions at the ground surface are computed using two different approaches: method (a), applying amplification factor to compute $Sa_{ij}(T)_{predicted}$, and method (b), applying GMPEs directly to derive $Sa_{ij}(T)_{predicted}$.

Method (a): Applying Amplification Factor (AF) to Compute $Sa_{ij}(T)_{predicted}$

In this method, the $Sa_{ij}(T)_{predicted}$ at ground surface were computed by modifying the predicted spectral accelerations at rock using the mean amplification factor (*AF*) values. *AF* values are transfer functions that can be defined for any ground motion parameters, but most commonly are assessed for acceleration response spectral values at different oscillator periods. In this current research, the *AF* values were defined using the ratio of surface-to-input spectral accelerations. The methodology proposed by Bazurro and Cornell (2004), was used to account for soil nonlinearity. The observed ground surface spectral accelerations are obtained from the site response analysis. Figures 24 and 25, shows the *AF* values versus period for the soft soil site and very stiff soil site, respectively. The *AF* values in these two plots were computed by using Equation 3 where, in this equation, $Sa_{ij}(T)_{observed\text{-}soil}$ values were obtained from the prediction of the site response analysis for each site:

$$AF = \frac{S_{ij}(T)_{observed-Soil}}{S_{ij}(T)_{observed-rock}} \quad (3)$$

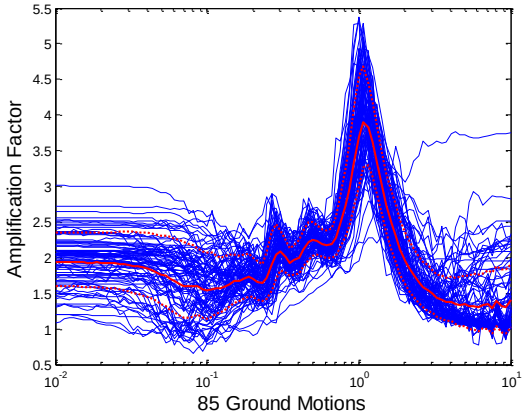

Figure 24. Amplification Factors versus periods for the soft soil site. The solid red line is the mean of all records, and the dotted red lines are the mean plus/minus one standard deviation.

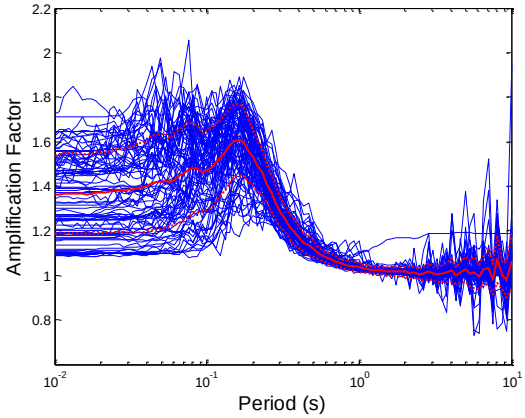

Figure 25. Amplification Factors versus periods for the stiff soil site. The solid red line is the mean of all records, and the dotted red lines are the mean plus/minus one standard deviation.

$Sa_{ij}(T)_{predicted}$ at the ground surface for each period were computed using the following equations:

$$ln\left[Sa_{ij}(T)_{predicted.soil}\right] = ln\left[Sa_{ij}(T)_{predicted.rock}\right] + \mu_{j\ ln(AF)} \quad (4)$$

$$\sigma_j(T)_{predicted.soil} = \sqrt{\sigma_{rock}{}^2 + \sigma_{ln(AF)}{}^2 + 2\,\rho_{ln\,(AF)ln\,S(rock)}\,\sigma_{rock}\,\sigma_{\ ln(AF)}} \quad (5)$$

where $Sa_{ij}(T)_{predicted.soil}$ are the predicted spectral accelerations for soil (after conducting site response analyses) at an oscillator period T at recording station i for event j; $Sa_{ij}(T)_{observed.rock}$ are the spectral accelerations predicted by a given GMPE for station i and event j (using the appropriate metadata); $\mu_{j\,ln(AF)}$ and $\sigma_{ln(AF)}$ are the mean and standard deviation of *ln(AF)* for each period over all stations; $\sigma_j(T)_{predicted.soil}$ is the standard deviation for soil site; σ_{rock} *i*s the standard deviation predicted by the GMPE over bedrock and $\rho_{ln\,(AF)\,S(rock)}$ is the correlation coefficient between *ln(AF)* and Sa_{rock}. The mean of *ln(AF)* , μ_j, and the standard deviation of *ln(AF)*, $\sigma_{\ ln(AF)}$, which were used in Equations 4 and 5,

respectively, are computed using the best curve fits through the scatter plot of AF values versus input Spectral acceleration at each single period between 0.01s and 10s for all ground motions.

SOFT SOIL SITE

Equation 6 (shown below) is obtained by regression analysis and presents the general best fit curves at each period and for all input motions for the soft soil site. Parameters a, b and c vary for each period in this regression model. Table 3A in the appendix A lists these parameters' values for the soft soil profile for all periods. The regression model plots for 6 different periods are shown in Figure 26.

$$Y = exp\ [a - b\ (ln[S_{ij}(T)_{observed.rock}]\ ) - c\ (ln[S_{ij}(T)_{observed.rock}])^{2}] \quad (6)$$

The models obtained from Equation 6 were modified for some cases. These modifications were applied based on some initial conditions. At some periods, the best curve fit plots were modified such that the section of the plot before the peak has AF values equal to the peak AF value (see Figures 26a-d). In this case, the input spectral acceleration at which the peak occurs corresponds to the onset of nonlinear behavior, and the assumption that the AF stays constant below this value is consistent with the assumption of linear behavior below the onset of nonlinearity. Also, at the periods such as those shown in Figures 26e-f, the best curve fit plots were assumed to be constants equal to the mean values of the AF scatter plot, due to the dispersed data; in other words, Equation 6 was not followed in these cases.

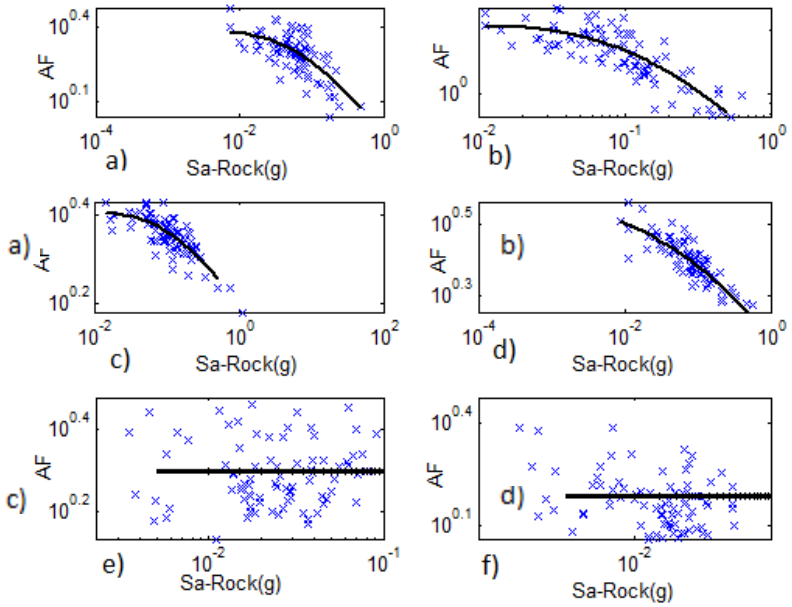

Figure 26. Regression model of AF versus $Sa(T)_{predicted.rock}$ for computing μ_j at a) T = 0.01s, b) T = 0.1 S, c) T = 0.5s, d) T = 0.75s, e) T = 2s and f) T = 3s.

Normalized residuals, $\epsilon_{ij}(T)$, were computed by using the observed and predicted spectral acceleration obtained by AF approach, as input data in Equation 1. Figure 27 shows the scatter plot of $\epsilon_{ij}(T)$ values versus 85 ground motions for two individual periods of 0.1s and 1s which includes the mean and the mean plus/minus one standard deviation as well (the black lines). Also, Figure 28 shows the mean and the standard deviation variation at each period for all ground motions. As is shown, there are the same shifts in mean $\epsilon_{ij}(T)$ values as can be seen in the same plot of rock $\epsilon_{ij}(T)$ values.

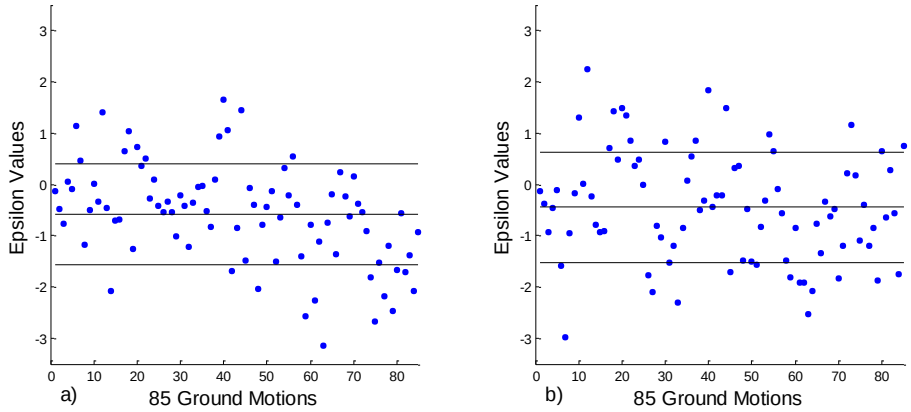

Figure 27. Scatter plot of $\epsilon_{ij}(T)$ for the 85 ground motions regarding the periods of a) T= 0.1s, and b) T= 1s. The black lines represent the mean and the mean plus/minus one standard deviation.

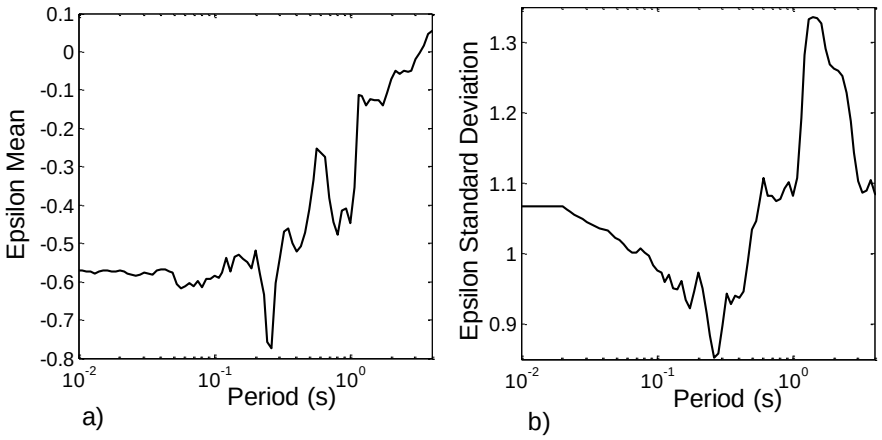

Figure 28. The mean and standard deviation of $\epsilon_{ij}(T)$ values versus period for soft soil site.

In order to explore the reason for the mean shift of the $\epsilon_{ij}(T)$ values versus period plot over the ground surface, the amplification factor (AF) epsilon values versus 85 ground motions for two individual periods of 0.1s and 1s which includes the mean and the mean plus/minus one standard deviation was constructed and is shown in Figure 29. As is illustrated, the AF epsilon values are unbiased and the slight $\epsilon_{ij}(T)$ mean values shift away from zero at the soil profile was due to the related mean shift at the bedrock plot (see Figures 20 and 21).

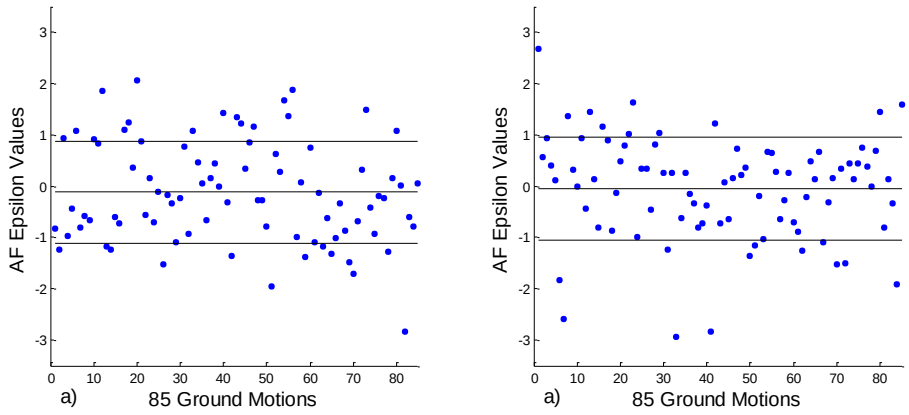

Figure 29. Scatter plot of AF $\epsilon_{ij}(T)$ values for the 85 ground motions regarding the periods of a) T= 0.1s, and b) T= 1s. The black lines represent the mean and the mean plus/minus one standard deviation.

The correlation structure of normalized residuals were also computed and plotted in Figure 30 below for 85 selected ground motions studied in this research. By comparing Figures 22 and 30, it can be seen that there is no significant difference between the correlation structures of residuals over the bedrock in comparison to the correlation structure of residuals after conducting site response analysis.

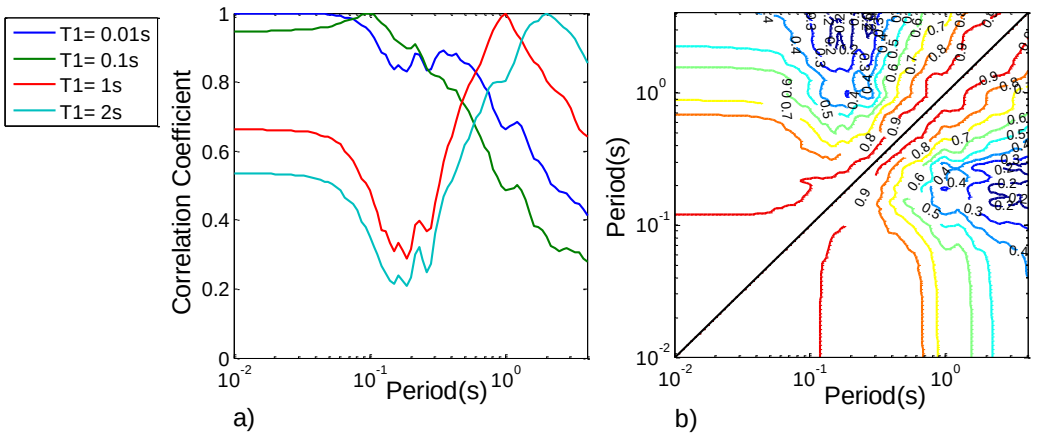

Figure 30. Correlation coefficients for soft soil site obtained using AS08. Correlation coefficients as (a) Selected periods (T_1) as a function of period (b) Contours.

VERY STIFF SOIL SITE:

In order to conduct the AF method for the stiff soil profile, the same procedure as for the soft soil profile was followed. However, for the stiff soil profile and the amplification factors are independent of the spectral acceleration at rock, hence the mean AF values at each period are used. This occurs because this site behaves largely linear for the selected input motions. Normalized residuals, $\epsilon_{ij}(T)$, were computed by using the observed and predicted spectral acceleration obtained by AF approach, as input data in Equation 1. Figure 31 shows the scatter plot of $\epsilon_{ij}(T)$ values versus 85 ground motions for two individual periods of 0.1s and 1s which includes the mean and the mean plus/minus one standard deviation as well (the black lines). Also, Figure 32 shows the mean and the standard deviation variation at each period for all ground motions. As can be seen there are the same shifts in mean $\epsilon_{ij}(T)$ values as were seen in the same plot for the bedrock.

Figure 31 shows the AF epsilon values versus 85 ground motions for two individual periods of 0.1s and 1s, as can be seen, the mean is unbiased as it was for the same plot at the soft soil profile. As is shown, we still can see some shift in the mean $\epsilon_{ij}(T)$ values over the ground surface for this profile, which is due to the related mean shift at the bedrock plot (see Figures 20 and 21). The shift in mean $\epsilon_{ij}(T)$ values at stiff soil profile is less than what we observed from the same plot at the soft soil profile (see Figures 27 and 28).

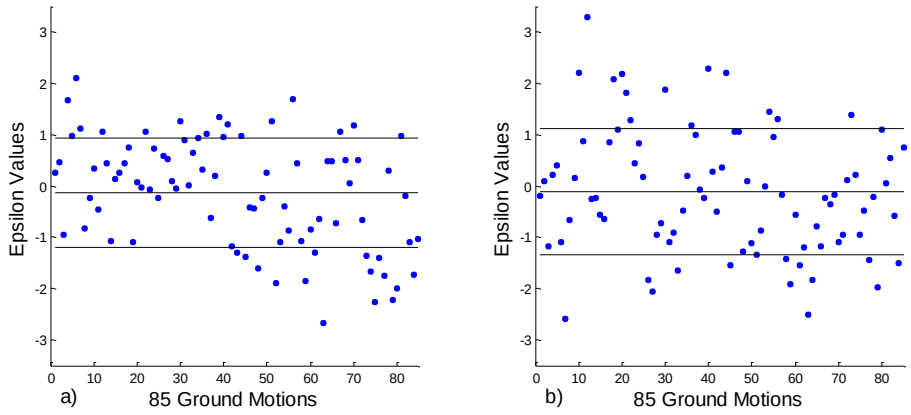

Figure 31.Scatter plot of $\epsilon_{ij}(T)$ for the 85 ground motions regarding the periods of a) T= 0.1s, and b) T= 1s. The black lines represent the mean and the mean plus/minus one standard deviation.

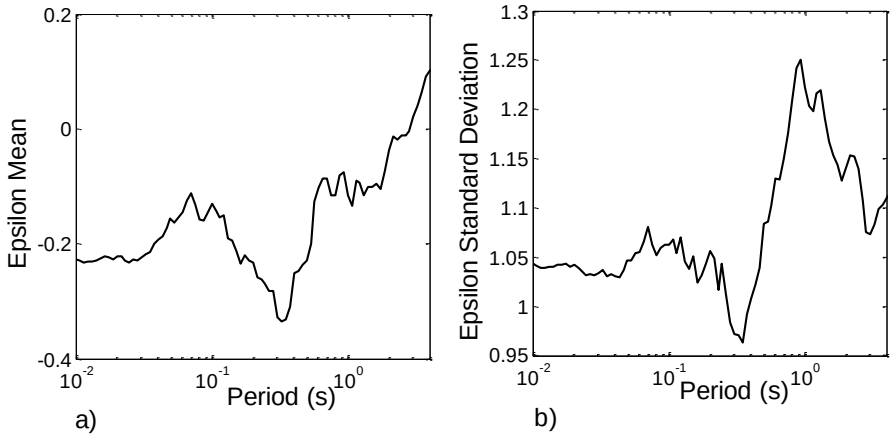

Figure 32. The mean and standard deviation of $\epsilon_{ij}(T)$ values versus period for stiff soil site.

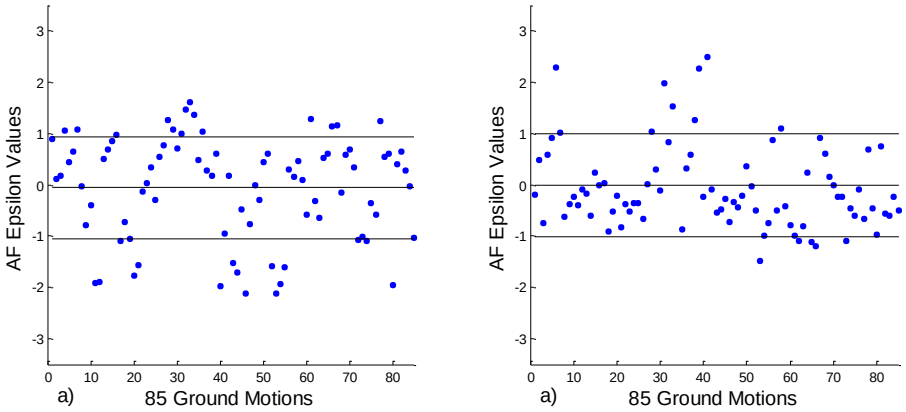

Figure 33. Scatter plot of AF $\epsilon_{ij}(T)$ values for the 85 ground motions regarding the periods of a) T= 0.1s, and b) T= 1s. The black lines represent the mean and the mean plus/minus one standard deviation.

The shift in mean $\epsilon_{ij}(T)$ values over the bedrock and consequently over the soft soil site (Bay area) can be due to the fact that the 85 selected ground motions used in this research may not be fully representative of the Abrahamson and Silva (2008) model.

The correlation structure of normalized residuals were computed and plotted in Figure 34 for the 85 selected ground motions. By comparing Figures 22 and 34, it can be seen that there is no significant difference between the correlation structures of residuals over the bedrock in comparison to the correlation structure of residuals after conducting site response analysis for the stiff soil site.

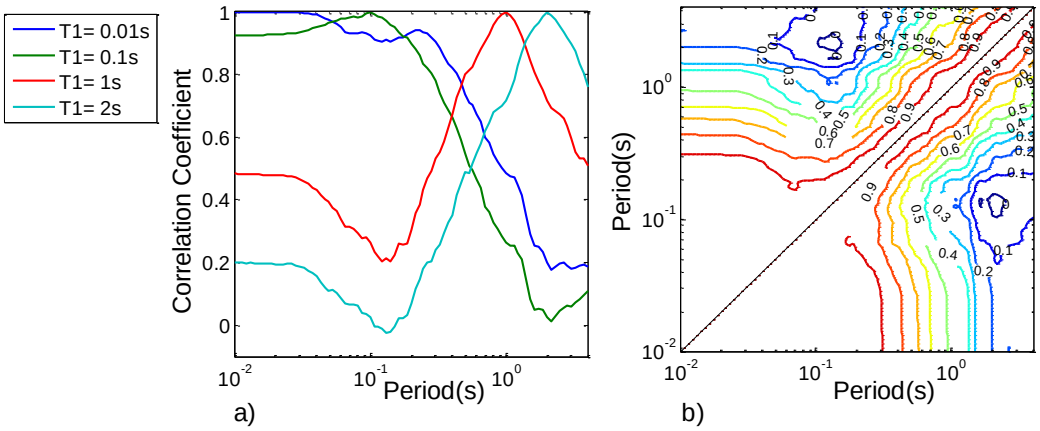

Figure 34. Correlation coefficients for stiff soil site obtained using AS08. Correlation coefficients as (a) Selected periods (T_1) as a function of period (b) Contours.

Method (b): Applying GMPEs directly to calculate $S_{ij}(T)_{predicted}$

The predicted spectral accelerations at the ground surface, $Sa_{ij}(T)_{predicted.soil}$, can also be computed through the three NGA models from Abrahamson and Silva (2008), Boore and Atkinson (2008) and Chiou and Young (2008). In order to obtain the spectral accelerations at their ground surface through the three mentioned NGA models, the shear wave velocity of the soil profiles at the top 30 m (Vs_{30}) needs to be used as input data, in these models. The computed Vs_{30} values are 132.5 m/s (434.7 ft/s) for the soft soil profile (see Figure 10) and 499.7 m/s (1639.45ft/s) for stiff soil profile (see Figure 15).

Normalized residuals, $\epsilon_{ij}(T)$, were computed by using the observed and predicted spectral accelerations obtained by NGA models, as input data in Equation 1. Figures 35 and 36 show the $\epsilon_{ij}(T)$ values versus the 85 ground motions along with $\epsilon_{ij}(T)$ values mean and standard deviation variation at each period for all ground motions for soft soil profile. As can be seen, the mean $\epsilon_{ij}(T)$ values shift significantly away from zero at long periods, which implies the GMPE method is not a reliable method for this soft soil site. Figures 37 and 38 show the same plots for the very stiff profile.

The shift in the mean $\epsilon_{ij}(T)$ values by conducting GMPE method is less for the stiff soil site in comparison to soft soil site. The reason for this difference can be due to this fact that the sites where the ground motions used to develop Abrahamson and Silva (2008) model were recorded were more similar to the stiff soil site in comparison to soft soil site.

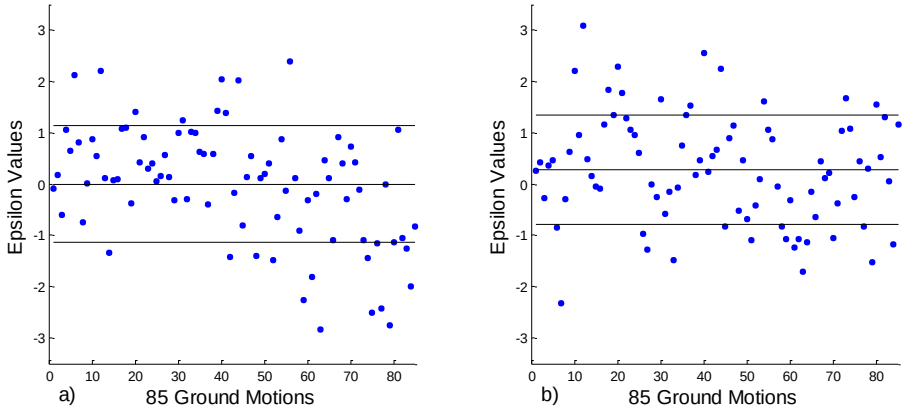

Figure 35. Scatter plot of $\epsilon_{ij}(T)$ for the 85 ground motions regarding the periods of a) T= 0.1s, and b) T= 1s. The black lines represent the mean and the mean plus/minus one standard deviation.

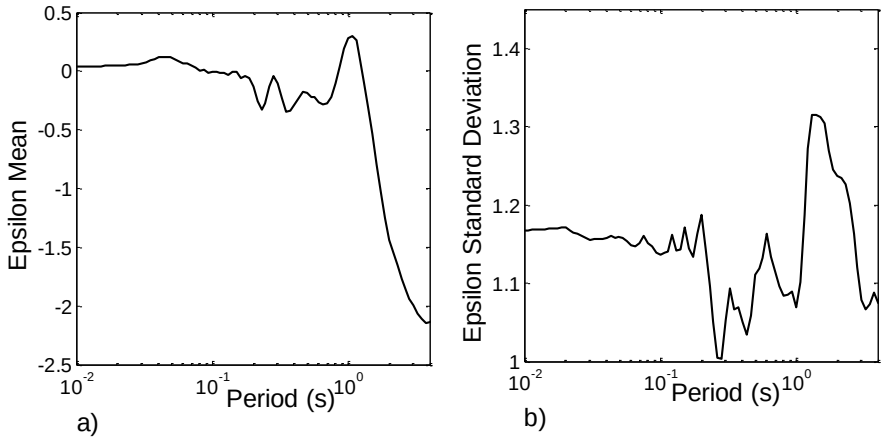

Figure 36. The mean and standard deviation of $\epsilon_{ij}(T)$ values versus period for soft soil site.

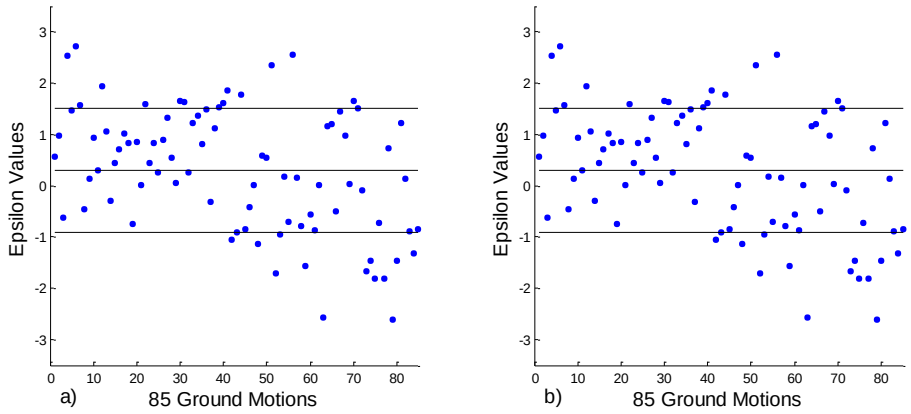

Figure 37. Scatter plot of $\epsilon_{ij}(T)$ for the 85 ground motions regarding the periods of a) T= 0.1s, and b) T= 1s. The black lines represent the mean and the mean plus/minus one standard deviation.

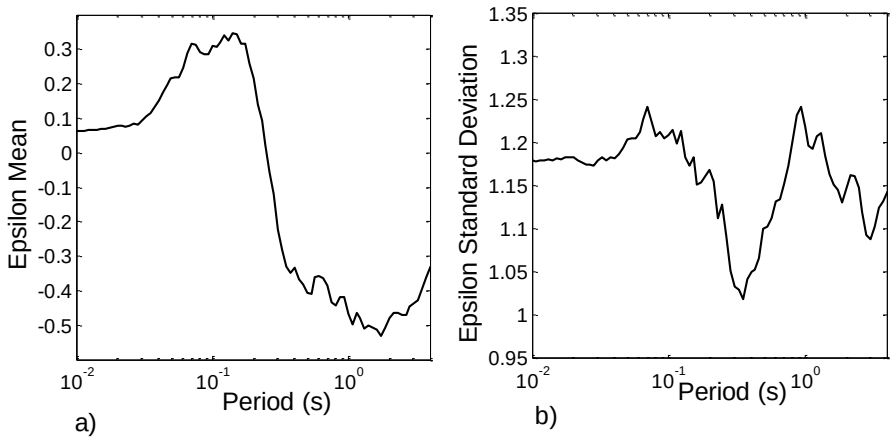

Figure 38. The mean and standard deviation of $\epsilon_{ij}(T)$ values versus period for stiff soil site.

The correlation structure of normalized residuals was computed for $\epsilon_{ij}(T)$ values applying GMPE approach. The obtained correlation structure of $\epsilon_{ij}(T)$ from method b is shown Figures 39 and 40 for soft soil site and stiff soil site, respectively. By comparing Figures 39 and 40 with Figure 22 ($\epsilon_{ij}(T)$ over bedrock) the same pattern can be seen within the correlation structure of $\epsilon_{ij}(T)$ values over bedrock and over soil sites using GMPE method (method b).

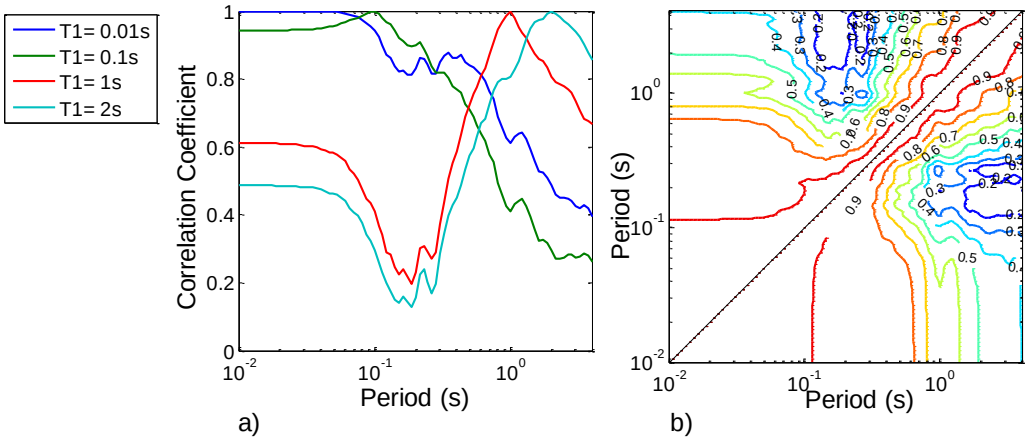

Figure 39. Correlation coefficients for soft soil site obtained using AS08. Correlation coefficients as (a) Selected periods (T_1) as a function of period (b) Contours.

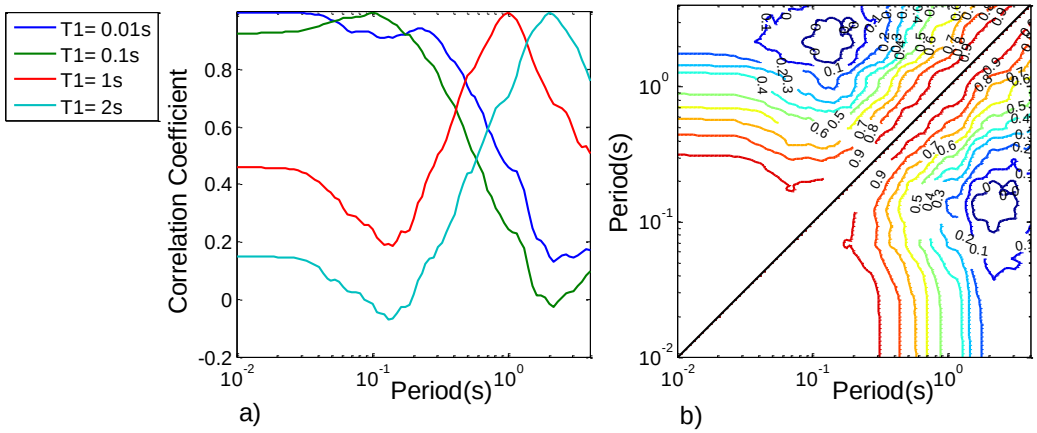

Figure 40. Correlation coefficients for stiff soil site obtained using AS08. Correlation coefficients as (a) Selected periods (T_1) as a function of period (b) Contours.

Figure 41 and 42 show the $Sa_{ij}(T)_{observed.soil}$ and the $Sa_{ij}(T)_{predicted.soil}$ values computed by applying methods (a) and (b) for the 1020 record measured during the 17 January 1994 Northridge earthquake for soft soil and stiff soil sites, respectively. As is shown, AF method yields closer prediction of soil spectral acceleration in comparison to GMPE method. Also, as can be seen the spectral acceleration values from AF method are higher for soft soil site in comparison to stiff soil site. This difference can be due to higher impedance contrast between bedrock and soft soil in comparison to very stiff soil. Figures 41 and 42 also show that there is higher amplification effects in the sites with lower resonance frequency (resonance frequency is 1 Hz for soft soil and 5 Hz for very stiff soil).

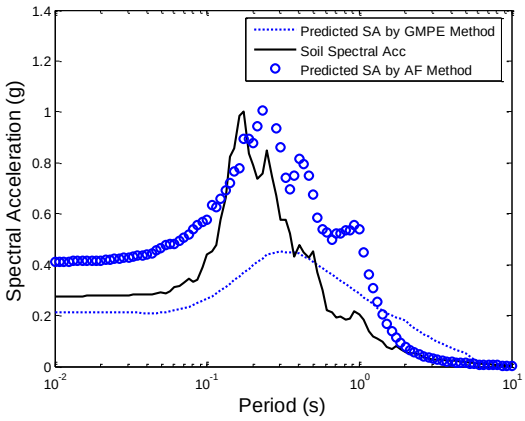

Figure 41. Plot of Soft Soil observed and Predicted Spectral Acceleration by method (a) and (b) For the 1020 record measured during the 17 January 1994 Northridge earthquake.

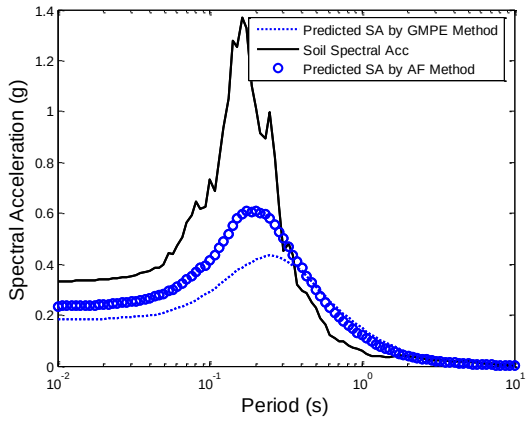

Figure 42. Plot of very stiff Soil observed and predicted spectral acceleration by method (a) and (b) For the 1020 record measured during the 17 January 1994 Northridge earthquake.

Figures 43 and 44 show the correlation structure of residuals over bedrock and after conducting site response analysis using methods (a) and (b) for periods of 0.01, 1, and 10 seconds. The black lines represent the correlation coefficients over bedrock, the red lines represent the correlation coefficients over the soil site using method (a) and the green lines represent the correlation coefficients over soil site using method (b). As can be seen the $\epsilon_{ij}(Ti)$ values have higher correlation with the ϵ_{ij} values at the T_i vicinity.

Figures 43 and 44 also indicate that although there is no significant difference between the shape of correlation coefficient contours for rock ground motions and contours after considering the effects of site response, there are some small differences. The correlation structure of residuals for shorter periods versus longer periods are higher for soft soil site with respect to bed rock. This is not observed for the very stiff soil site. The correlation structure is lower for stiff soil in respect to bedrock in those periods.

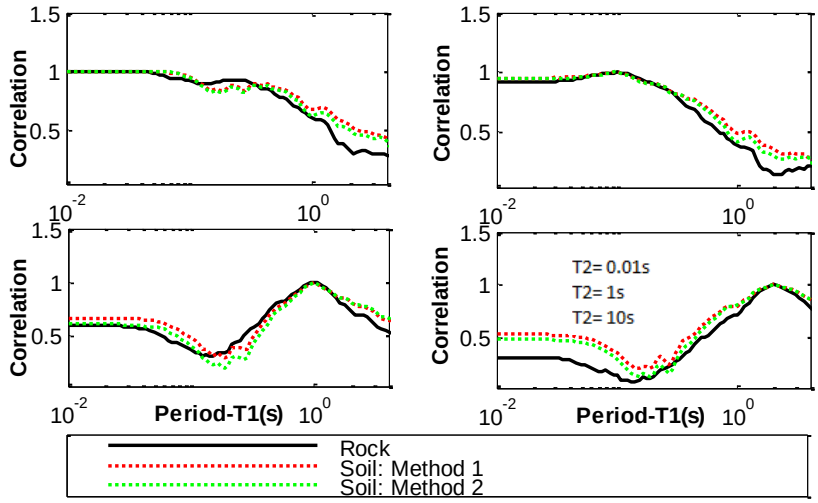

Figure 43. Comparison of the correlation structure for 4 periods for the soft soil site using the two proposed methods in this study.

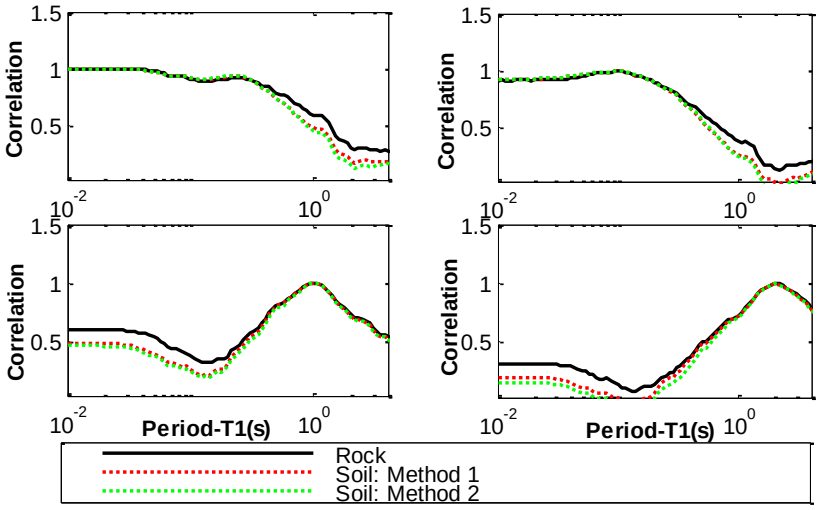

Figure 44. Comparison of the correlation structure for 4 periods for the soft stiff site using the two proposed methods in this study.

CONCLUSION

In this paper, we explore the effects of site response on the correlation structure of ground motion residuals over bedrock using two hypothetical soil profiles: soft soil site and very stiff site. Results indicate that there is no significant difference between the shape of correlation coefficient contours for rock ground motions and contours after considering the effects of site response. However, there are some differences. The correlation structure of residuals for shorter periods versus longer periods are higher for soft soil site with respect to bed rock. This is not observed for the very stiff soil site. The correlation structure is lower for stiff soil in respect to bedrock in those periods.

Based on the comparison of predicted spectral accelerations from AF method and GMPE method, it can be concluded that GMPE method is not the best method to predict the spectral acceleration values over the ground surface for very soft soils. This can be due to the fact that the accuracy of the computed spectral acceleration values from GMPE method depends on the similarity of given site with the sites in the database of ground motions used to derive the GMPE which is being used, whereas, AF method computes spectral acceleration values considering the given soil site directly.

REFERENCES

Abrahamson, N., Atkinson, G., Boore, D., Bozorgnia, Y., Campbell, K., Chiou, B., Idriss, I. M., Silva, W., and Youngs, R. (2008). "Comparisons of the NGA Ground-Motion Relations." Earthquake Spectra": February 2008, Vol. 24, No. 1, pp. 45-66

Abrahamson, N., and Silva, W. (2008). "Summary of the Abrahamson & Silva NGA ground motion Relations", Earthquake Spectra 24 , 67–97.

Baker, J. (2011). "Conditional Mean Spectrum: Tool for Ground-Motion Selection." Journal of Structural. Engineering. 137, SPECIAL ISSUE: Earthquake Ground Motion Selection and Modification for Nonlinear Dynamic Analysis of Structures, 322–331.

Baker, J., and Cornell, C. (2006). "Correlation of Response Spectral Values for Multicomponent Ground Motions." Bulletin of the Seismological Society of America 96(1), 215-227.

Baker, J. and Jayaram, N. (2008). "Correlation of Spectral Acceleration Values from NGA Ground Motion Models." Earthquake Spectra 24(1), 299-317.

Bazurro, P. and Cornell, C. (2004). "Nonlinear Soil-site Effects in Probabilistic Seismic Hazard Analysis." Bulletin of the Seismological Society of America 94(6), 2110-2123.

Boore, D. and Atkinson, G. (2008). " Ground-Motion Prediction Equations for the Average Horizontal Component of PGA, PGV, and 5%-Damped PSA at Spectral Periods between 0.01 s and 10.0 s." Earthquake Spectra: February 2008, Vol. 24, No. 1, pp. 99-138.

Bradley, B. (2012). "Empirical Correlations Between Peak Ground Velocity and Spectrum-Based Intensity Measures." Earthquake Spectra, 28(1), 17-35.doi:10.1193/1.3675582

Chiou, B. S. J., and Youngs, R. R. (2008). "Chiou-Youngs NGA Ground Motion Relations for the Geometric Mean Horizontal Component of Peak and Spectral Ground Motion Parameters", Earthquake Spectra 24 , 173–215.

EPRI (1993). "Guidelines for Determining Design Basis Ground Motions." Electric Power Research Institute, EPRI TR-012293s, Palo Alto, CA

Finn, W. D. L. (1991). " Geotechnical engineering aspects of microzonation." Paper presented at the 199-259.

Idriss, I. M. and Sun, J. I. (1992). "User's Manual for SHAKE91, A computer Program for Conducting Equivalent Linear Seismic Response Analyses of Horizontally Layered Soil Deposits Program Modified based on the Original SHAKE Program Published in December 1972 by Schnabel, Lysmer and Seed."

Isenhower, W. M., and Stokoe, K. H. II (1981). "Strain-rate dependent shear modulus of San Francisco Bay mud." International Conference on Recent Advances in Geotechnical Earthquake Engineering, University of Missouri,, Rolla, pp. 597- 602.

Kalkan, E., Wills, C. J., and Branum, D. M. (2008). “Seismic Hazard Mapping of California Incorporating Spatial Variability of Site Conditions.” In Proc. of the East Bay Conference.

Kottke, R. A. and Rathje, M. E. (2008). “ Technical Manual for Strata.” Pacific Earthquake Engineering Research Center College of Engineering University of California, Berkeley, October 2008.

Kramer, S. L. (1996). Geotechnical Earthquake Engineering. Upper Saddle River, NJ: Prentice-Hall, Inc.

Mohraz, B. (1976), “Earthquake Response Spectra for Different Geologic Conditions. ” Bulletin of the Seismological Society of America, 66, 915-935.

Pacific Earthquake Engineering Research Center: NGA Database.(2005). Pacific Earthquake Engineering Center, Berkeley, California. Retrieved from http://peer.berkeley.edu/nga/

Power, M., Chiou, B., Abrahamson, N., Bozorgnia, Y., Shantz, T., and Roblee, C. (2008). “An Overview of the NGA Project.” Earthquake Spectra 24(1), 3-21.

Rodriguez- Marek, A. (2000). “Near-Fault Seismic Site Response” University of California, Berkeley, ProQuest, UMI Dissertations Publishing, 2000. 3002238.

Seed, H. B. and Idriss, I. M. (1969). “The Influence of Soil Conditions on Ground Motions During Earthquakes.” Journal of the Soil Mechanics and Foundation Engineering Division, ASCE , No. 94, 93-137.

Seed, H. B., and Idriss, I. M. (1983). "Ground motions and soil liquefaction during earthquakes." EERI Monograph Series, Earthquake Engineering Research Institute, Berkeley, CA.

Seed, H. B., Ugas, C., and Lysmer, J. (1976). “Site Dependent Spectra for Earthquake Resistant Design.” Bulletin of the Seismological Society of America, 66, 221-244.

Sykora, D. W, Moriwaki, Y, and Barneich, J.A. (1996). “Measured variation of peak acceleration and peak particle velocity with depth at soil sites.” Paper presented at the

Vucetic, M., and Dobry, R. (1991). "Effect of Soil Plasticity on Cyclic Response." Journal of Geotechnical Engineering, ASCE, Vol. 117(1).

CHAPTER 4

CONCLUSION AND ENGINEERING SIGNIFICANCE

Seismic hazard analyses require an estimate of earthquake ground motions from future events. These predictions are achieved through Ground Motion Prediction Equations, which include a prediction of the median and the standard deviation of ground motion parameters. For spectral accelerations, the correlation structure of normalized residuals across oscillator periods is important for guiding ground motion selection. Correlation structures of $\epsilon_j(T)$ for a large global dataset have been studied extensively. These correlation structures reflect effects that are averaged over the entire dataset underlying the analyses.

In this thesis, we explore the effects of site response on the correlation structure of ground motion residuals over bedrock using a set of 85 rock input motions and two hypothetical soil profiles: soft soil site and very stiff site. Correlation structures of $\epsilon_j(T)$ for a large global dataset have been studied extensively. These correlation structures reflect effects that are averaged over the entire dataset underlying the analyses.

Although it was expected to have a marked effect of site response on the correlation structure for the site profile under study, based on the result, there is no significant difference between the shape of correlation coefficient contours for rock ground motions and contours after considering the effects of site response. However, correlation structure of residuals for shorter periods versus longer periods are more evidently higher for soft soil site in respect to bed rock whereas, it is not true for very stiff soil site and the correlation structure is higher for stiff soil in respect to bedrock in those periods.

Moreover, based on the comparison of predicted spectral accelerations from AF method and GMPE method, it can be concluded that GMPE method is not the best method to predict the spectral acceleration values over the ground surface. This can be due to the fact that the accuracy of the computed spectral acceleration values from GMPE method depends on the similarity of given site with the ground motion sources used to derive the GMPE which is being used, whereas, AF method computes spectral acceleration values considering the given soil site directly.

RECOMMENDATIONS FOR FUTURE WORK

Soil nonlinearity is the source of many uncertainties in geotechnical field since early years. These doubts are more noticeable when dynamic behavior of soil is investigated. Since it is very complicated to predict the dynamic behavior of soil, if it is not impossible, statistical methods are used significantly in this field as tools to explore and predict soil behavior.

Dynamic soil behavior is based on some basic properties of soil and site such as shear wave velocity of soil and the site's impedance contrast; therefore use of different soil profiles with different properties to conduct site response analyses for each research topic can improve the results' and conclusions' reliability level.

Also, use of various statistical methods as tools to compare the results of the analyses, such as correlation coefficients or regression methods (which are applied in this current research) would be a right track to follow for the future work. For instance use of some other soil profiles with different properties in this current research along with apply other statistical methods to compare the result could help to derive more comprehensive conclusions.

Choosing ground motions which are fully representative of ground motion prediction equations GMPEs are highly recommended for ground motion selection purposes in seismic analyses. Also, use of other methods to predict soil spectral accelerations can lead to different result.

APPENDIX A – SUPPORTIVE FIGURES AND METADATA

In the appendix some plots regarding the results of this current research is presented with the aim of better understanding this research's subject. Figures 1 through 18 show the acceleration time histories of few ground motions, selected from the 85 ground motions used in this research, for both rock and soft soil site that illustrate the site effect on the input ground motions. Also, Figures 19 through 22 present the input ground motions of this research metadata introduced in Table 1A, by using different distribution plots. Figures 19 and 20 present the Vs_{30} and *PGA* histograms. The frequency of ground motions selected from each event is shown in Table 3A in the appendix A. Figure 21 shows the earthquake magnitude (*Mw*) versus the closest distance from the recording site to the ruptured area (ClstD in km) and Figure 22 depicts the Vs_{30} versus *PGA* (g). The presented figures illustrate a fairly uniform selection of ground motions.

Table 1A. Metadata table for 85 ground motions of 14 different earthquakes.

Record Sequence Number	Earthquake Name	Earthquake Magnitude	Dip (deg)	Rake Angle (deg)	Depth to Top Of Fault Rupture Model	Joyner-Boore Dist. (km)	ClstD (km)	Rx	Vs30 (m/s) selected for analysis	Fault Rupture Width (km)	Frv	Fnm	Fhw	Fvs30	irock	Z1 (As)
59	San Fernando	6.61	50	83	0.00	89.37	89.72	22.28	813.48	27.41	1	0	0	0	1	24.87
63	San Fernando	6.61	50	83	0.00	25.58	30.19	34.4	634.33	27.41	1	0	0	0	1	53.74
67	San Fernando	6.61	50	83	0.00	130	130.98	131.22	591	27.41	1	0	0	0	1	53.74
72	San Fernando	6.61	50	83	0.00	19.45	25.07	27.13	600.06	27.41	1	0	0	0	1	23.77
80	San Fernando	6.61	50	83	0.00	21.5	21.5	11.98	969.07	27.41	1	0	0	0	1	11.35
87	San Fernando	6.61	50	83	0.00	30.7	30.7	4.38	667.13	27.41	1	0	0	0	1	53.74
89	San Fernando	6.61	50	83	0.00	61.75	63.79	46.82	669.48	27.41	1	0	0	0	1	59.52
283	Irpinia, Italy-01	6.9	60	-90	0.80	52.93	52.94	25.29	612.78	15.00	0	1	0	0	1	9.86
293	Irpinia, Italy-01	6.9	60	-90	0.80	59.63	59.63	48.57	593.35	15.00	0	1	0	0	1	63.62
369	Coalinga-01	6.36	30	90	3.00	25.98	27.46	35.51	648.09	11.00	1	0	0	0	1	53.74
748	Loma Prieta	6.93	70	140	3.00	43.94	44.11	13.26	627.59	18.00	1	0	0	0	1	79.50
771	Loma Prieta	6.93	70	140	3.00	79.71	79.81	30.28	584.17	18.00	1	0	0	0	1	62.04
774	Loma Prieta	6.93	70	140	3.00	54.97	55.11	40.16	735.44	18.00	1	0	0	0	1	72.04
775	Loma Prieta	6.93	70	140	3.00	29.54	30.24	5.16	621.2	18.00	1	0	0	0	1	39.07
781	Loma Prieta	6.93	70	140	3.00	48.24	48.39	11.9	586.08	18.00	1	0	0	0	1	53.74
782	Loma Prieta	6.93	70	140	3.00	39.69	44.35	44.71	638.63	18.00	1	0	0	0	1	44.94
788	Loma Prieta	6.93	70	140	3.00	72.9	73	44.44	895.36	18.00	1	0	0	0	1	53.74
789	Loma Prieta	6.93	70	140	3.00	83.37	83.45	28.78	1315.92	18.00	1	0	0	0	1	16.18
791	Loma Prieta	6.93	70	140	3.00	33.94	34.32	3.39	608.67	18.00	1	0	0	0	1	2.88
793	Loma Prieta	6.93	70	140	3.00	78.58	78.68	25.65	614.57	18.00	1	0	0	0	1	53.74
795	Loma Prieta	6.93	70	140	3.00	75.96	76.05	31.22	1249.86	18.00	1	0	0	0	1	44.94
797	Loma Prieta	6.93	70	140	3.00	74.04	74.14	32.91	873.1	18.00	1	0	0	0	1	3.63
798	Loma Prieta	6.93	70	140	3.00	76.4	76.5	33.49	585.23	18.00	1	0	0	0	1	18.11
804	Loma Prieta	6.93	70	140	3.00	63.03	63.15	23.29	1020.62	18.00	1	0	0	0	1	44.94
813	Loma Prieta	6.93	70	140	3.00	75.07	75.17	36.37	659.81	18.00	1	0	0	0	1	9.00
891	Landers	7.28	90	180	0.00	50.85	50.85	40.94	659.09	14.99	0	0	0	0	1	63.53
897	Landers	7.28	90	180	0.00	41.43	41.43	37.99	635.01	14.99	0	0	0	0	1	53.74
943	Northridge-01	6.69	40	103	5.00	65.84	68.93	72.11	501.75	24.00	1	0	0	0	1	53.74
946	Northridge-01	6.69	40	103	5.00	46.65	46.91	46.52	572.57	24.00	1	0	0	0	1	23.77
994	Northridge-01	6.69	40	103	5.00	21.2	23.77	10.77	1015.88	24.00	1	0	0	0	1	23.77
1020	Northridge-01	6.69	40	103	5.00	20.77	21.36	19.21	602.1	24.00	1	0	0	0	1	9.19
1021	Northridge-01	6.69	40	103	5.00	31.27	31.66	30.65	600.06	24.00	1	0	0	0	1	95.73
1023	Northridge-01	6.69	40	103	5.00	24.86	25.36	22.8	670.84	24.00	1	0	0	0	1	23.77
1041	Northridge-01	6.69	40	103	5.00	35.53	35.88	11.08	680.37	24.00	1	0	0	0	1	23.77
1060	Northridge-01	6.69	40	103	5.00	79.83	79.99	29.5	509.1	24.00	1	0	0	0	1	23.77
1091	Northridge-01	6.69	40	103	5.00	23.1	23.64	23.1	996.43	24.00	1	0	0	0	1	23.77
1096	Northridge-01	6.69	40	103	5.00	64.46	64.66	41.59	662.7	24.00	1	0	0	0	1	10.02
1109	Kobe, Japan	6.9	85	180	0.20	69.04	70.26	56.2	609	20.00	0	0	0	0	1	23.77
1112	Kobe, Japan	6.9	85	180	0.20	86.93	86.94	74.31	609	20.00	0	0	0	0	1	90.97
1117	Kobe, Japan	6.9	85	180	0.20	119.64	119.64	117.82	609	20.00	0	0	0	0	1	90.97
1123	Kozani, Greece-01	6.4	43	-95	2.00	72.82	74.06	84.3	649.67	15.70	0	1	0	0	1	90.97
1125	Kozani, Greece-01	6.4	43	-95	2.00	47.79	49.66	59.27	579.4	15.70	0	1	0	0	1	63.62
1154	Kocaeli, Turkey	7.51	80	180	0.00	65.53	65.53	55.49	612.78	20.25	0	0	0	0	1	63.62
1159	Kocaeli, Turkey	7.51	80	180	0.00	141.37	142.29	49	585.09	20.25	0	0	0	0	1	63.62
1219	Chi-Chi, Taiwan	7.62	30	55	0.00	56.93	57.5	16.15	602.63	40.22	1	0	0	0	1	63.62
1257	Chi-Chi, Taiwan	7.62	30	55	0.00	52.46	56.14	85.38	1525.85	40.22	1	0	0	0	1	95.35
1278	Chi-Chi, Taiwan	7.62	30	55	0.00	50.47	54.29	85.41	614.05	40.22	1	0	0	0	1	1.49
1287	Chi-Chi, Taiwan	7.62	30	55	0.00	37.54	42.54	71.39	642.73	40.22	1	0	0	0	1	87.66
1293	Chi-Chi, Taiwan	7.62	30	55	0.00	47.79	51.8	81.59	617.52	40.22	1	0	0	0	1	71.45
1325	Chi-Chi, Taiwan	7.62	30	55	0.00	80.88	83.31	84.92	649.25	40.22	1	0	0	0	1	85.48
1347	Chi-Chi, Taiwan	7.62	30	55	0.00	57.69	61.06	54.25	996.51	40.22	1	0	0	0	1	68.29
1352	Chi-Chi, Taiwan	7.62	30	55	0.00	113.39	114.44	30.84	913.77	40.22	1	0	0	0	1	10.02
1440	Chi-Chi, Taiwan	7.62	30	55	0.00	120.84	122.48	57.88	1023.45	40.22	1	0	0	0	1	14.77
1441	Chi-Chi, Taiwan	7.62	30	55	0.00	114.15	115.34	33.08	662.78	40.22	1	0	0	0	1	8.89
1446	Chi-Chi, Taiwan	7.62	30	55	0.00	117.31	119	68.35	1022.77	40.22	1	0	0	0	1	62.26
1485	Chi-Chi, Taiwan	7.62	30	55	0.00	26	26	0.61	704.64	40.22	1	0	0	0	1	8.92
1518	Chi-Chi, Taiwan	7.62	30	55	0.00	55.14	58.09	36.8	999.66	40.22	1	0	0	0	1	47.32
1577	Chi-Chi, Taiwan	7.62	30	55	0.00	62.67	65.79	82.3	704.96	40.22	1	0	0	0	1	9.88
1585	Chi-Chi, Taiwan	7.62	30	55	0.00	43.99	48.33	77.3	728.01	40.22	1	0	0	0	1	47.23
1587	Chi-Chi, Taiwan	7.62	30	55	0.00	62.11	65.25	93.46	845.34	40.22	1	0	0	0	1	40.89
1613	Duzce, Turkey	7.14	65	182	0.00	25.78	25.88	2.54	782	20.28	0	0	0	0	1	20.93
1619	Duzce, Turkey	7.14	65	182	0.00	34.3	34.3	34.3	535.24	20.28	0	0	0	0	1	29.68
1625	Sitka, Alaska	7.68	90	180	0.00	106.71	106.71	105.37	521.76	15.00	0	0	0	0	1	63.62
1626	Sitka, Alaska	7.68	90	180	0.00	34.61	34.61	34.61	649.67	15.00	0	0	0	0	1	63.62
1763	Hector Mine	7.13	77	179	0.00	89.98	89.98	74.21	724.89	16.20	0	0	0	0	1	63.62
1767	Hector Mine	7.13	77	179	0.00	83.43	83.43	83.16	667.42	16.20	0	0	0	0	1	53.74
1786	Hector Mine	7.13	77	179	0.00	61.21	61.21	61.21	624.94	16.20	0	0	0	0	1	53.74
1795	Hector Mine	7.13	77	179	0.00	50.42	50.42	31.94	686.12	16.20	0	0	0	0	1	53.74
1824	Hector Mine	7.13	77	179	0.00	96.91	96.91	93.45	642.83	16.20	0	0	0	0	1	53.74
1832	Hector Mine	7.13	77	179	0.00	87.2	87.2	86.36	564.93	16.20	0	0	0	0	1	63.62
1836	Hector Mine	7.13	77	179	0.00	42.06	42.06	13.5	635.01	16.20	0	0	0	0	1	53.74
3292	Chi-Chi, Taiwan-06	6.3	30	100	10.00	82.87	83.47	39.43	602.63	20.00	1	0	0	0	1	95.35
3325	Chi-Chi, Taiwan-06	6.3	30	100	10.00	52.33	56.02	63.73	1525.85	20.00	1	0	0	0	1	1.49
3342	Chi-Chi, Taiwan-06	6.3	30	100	10.00	49.18	53.09	66.5	614.05	20.00	1	0	0	0	1	87.66
3350	Chi-Chi, Taiwan-06	6.3	30	100	10.00	41.34	45.92	48.38	642.73	20.00	1	0	0	0	1	71.45
3355	Chi-Chi, Taiwan-06	6.3	30	100	10.00	56.84	60.25	69.52	617.52	20.00	1	0	0	0	1	85.48
3390	Chi-Chi, Taiwan-06	6.3	30	100	10.00	82.06	84.47	54.36	996.51	20.00	1	0	0	0	1	10.02
3472	Chi-Chi, Taiwan-06	6.3	30	100	10.00	23.84	25.85	23.84	614.98	20.00	1	0	0	0	1	87.07
3479	Chi-Chi, Taiwan-06	6.3	30	100	10.00	81	83.43	37.67	999.66	20.00	1	0	0	0	1	9.88
3489	Chi-Chi, Taiwan-06	6.3	30	100	10.00	34.02	35.46	22.51	714.27	20.00	1	0	0	0	1	44.53
3507	Chi-Chi, Taiwan-06	6.3	30	100	10.00	22.69	24.8	22.69	511.18	20.00	1	0	0	0	1	61.57
3509	Chi-Chi, Taiwan-06	6.3	30	100	10.00	32.11	33.63	32.11	652.85	20.00	1	0	0	0	1	66.62
3532	Chi-Chi, Taiwan-06	6.3	30	100	10.00	91.9	94.02	26.1	704.96	20.00	1	0	0	0	1	47.23
3540	Chi-Chi, Taiwan-06	6.3	30	100	10.00	65.87	68.84	36.54	728.01	20.00	1	0	0	0	1	40.89
3542	Chi-Chi, Taiwan-06	6.3	30	100	10.00	84.03	86.38	46.05	845.34	20.00	1	0	0	0	1	20.93

Table 2A. Data base earthquakes names and their frequencies

Earthquake Name	EQ Frequency
San Fernando	7
Irpinia, Italy-01	2
Coalinga-01	1
Loma Prieta	15
Landers	2
Northridge-01	10
Kobe, Japan	3
Kozani, Greece-01	2
Kocaeli, Turkey	2
Chi-Chi, Taiwan	16
Duzce, Turkey	2
Sitka, Alaska	2
Hector Mine	7
Chi-Chi, Taiwan-06	14

Table 3A. Coefficients for the regression model presented at equation 6.

T (s)	**a**	**b**	**c**
0.01000	-0.08939	-0.38302	-0.03798
0.01072	-0.08533	-0.38155	-0.03786
0.01150	-0.07641	-0.37722	-0.03730
0.01233	-0.07852	-0.37730	-0.03721
0.01322	-0.07835	-0.37573	-0.03679
0.01417	-0.08301	-0.37762	-0.03706
0.01520	-0.09199	-0.38233	-0.03775
0.01630	-0.10232	-0.38671	-0.03818
0.01748	-0.10416	-0.38988	-0.03884
0.01874	-0.10766	-0.39541	-0.03995
0.02009	-0.12377	-0.40273	-0.04082
0.02154	-0.13963	-0.40980	-0.04163
0.02310	-0.14609	-0.41635	-0.04278
0.02477	-0.15287	-0.42262	-0.04398
0.02656	-0.18847	-0.44252	-0.04672
0.02848	-0.18600	-0.44132	-0.04669
0.03054	-0.25276	-0.48202	-0.05274
0.03275	-0.27123	-0.48652	-0.05272
0.03511	-0.26166	-0.47934	-0.05168
0.03765	-0.31436	-0.51208	-0.05678
0.04037	-0.32226	-0.51409	-0.05688
0.04329	-0.32882	-0.51336	-0.05662
0.04642	-0.36963	-0.52921	-0.05800
0.04977	-0.36842	-0.51267	-0.05402
0.05337	-0.42562	-0.54471	-0.05866
0.05722	-0.56599	-0.63050	-0.07173
0.06136	-0.67253	-0.69894	-0.08318

0.06579	-0.74193	-0.73656	-0.08835
0.07055	-0.75275	-0.73538	-0.08771
0.07565	-0.68982	-0.69313	-0.08172
0.08111	-0.64302	-0.66881	-0.07874
0.08697	-0.57472	-0.63300	-0.07473
0.09326	-0.60547	-0.64617	-0.07706
0.10000	-0.62370	-0.66828	-0.08217
0.10723	-0.49669	-0.58803	-0.06822
0.11498	-0.44210	0	0
0.12328	-0.33612	0	0
0.13219	-0.28786	0	0
0.14175	-0.19935	0	0
0.15199	-0.09641	0	0
0.16298	-0.05782	0	0
0.17475	0.04397	0	0
0.18738	0.09194	0	0
0.20092	0.13933	0	0
0.21544	0.15142	0	0
0.23101	0.15536	0	0
0.24771	0.14368	0	0
0.26561	0.10214	0	0
0.28480	0.12033	0	0
0.30539	0.29496	0	0
0.32745	0.35343	0	0
0.35112	0.32176	0	0
0.37649	0.33410	0	0
0.40370	0.34070	0	0
0.43288	0.34046	0	0
0.46416	0.37439	0	0
0.49770	0.43839	0	0
0.53367	0.44785	0	0
0.57224	0.48209	0	0
0.61359	0.56892	0	0
0.65793	0.53606	0	0
0.70548	0.54175	0	0
0.75646	0.42825	0	0
0.81113	0.37165	0	0
0.86975	0.37108	0	0
0.93260	0.39899	0	0
1.00000	0.37005	0	0
1.07227	0.32772	0	0
1.14976	0.54507	0	0
1.23285	0.75429	0	0
1.32194	1.01970	0	0
1.41747	1.32990	0	0
1.51991	1.45280	0	0
1.62975	1.53310	0	0
1.74753	1.48570	0	0
1.87382	1.56780	0	0
2.00923	1.47710	0	0
2.15443	1.53670	0	0

2.31013	1.79700	0	0
2.47708	1.80790	0	0
2.65609	1.77230	0	0
2.84804	1.90570	0	0
3.05386	1.77890	0	0
3.27455	1.57300	0	0
3.51119	1.43870	0	0
3.76494	1.59850	0	0
4.03702	1.08310	0	0
4.32876	0.67344	0	0
4.64159	0.27513	0	0
4.97702	-0.10130	0	0
5.33670	-0.42225	0	0
5.72237	-0.56929	0	0
6.13591	-0.78030	0	0
6.57933	-0.64050	0	0
7.05480	-0.90169	0	0
7.56463	-1.15760	0	0
8.11131	-0.88280	0	0
8.69749	-1.32620	0	0
9.32603	-1.23240	0	0
10.00000	-1.02680	0	0

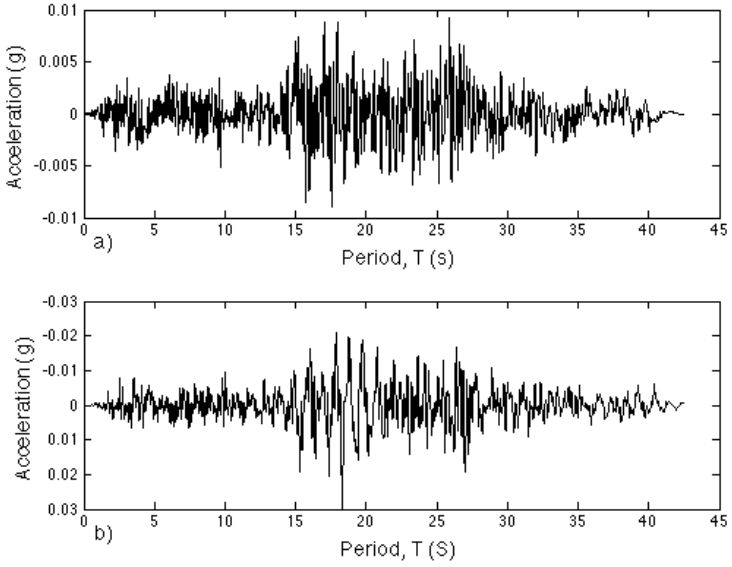

Figure A1. Acceleration time history a) over bedrock b) over soil layer for the February 9th, 1971 San Fernando earthquake (Record sequence No of 67.)

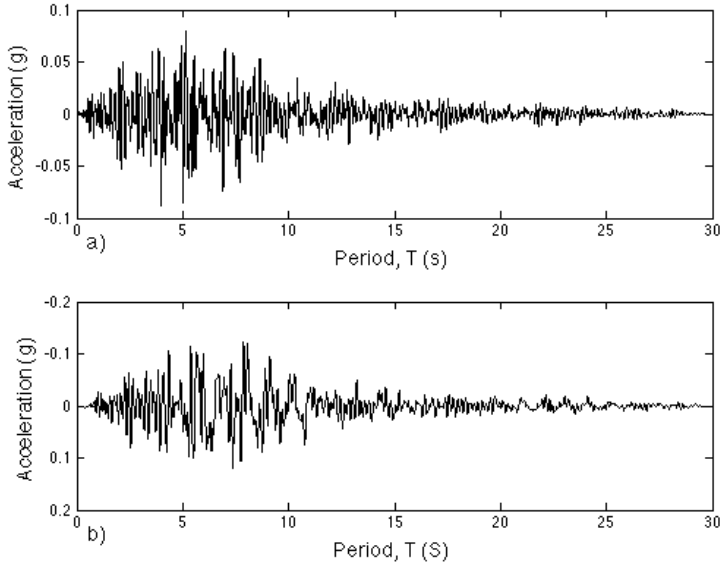

Figure A2. Acceleration time history a) over bedrock b) over soil layer for the February 9th, 1971 San Fernando earthquake (Record sequence No of 80.)

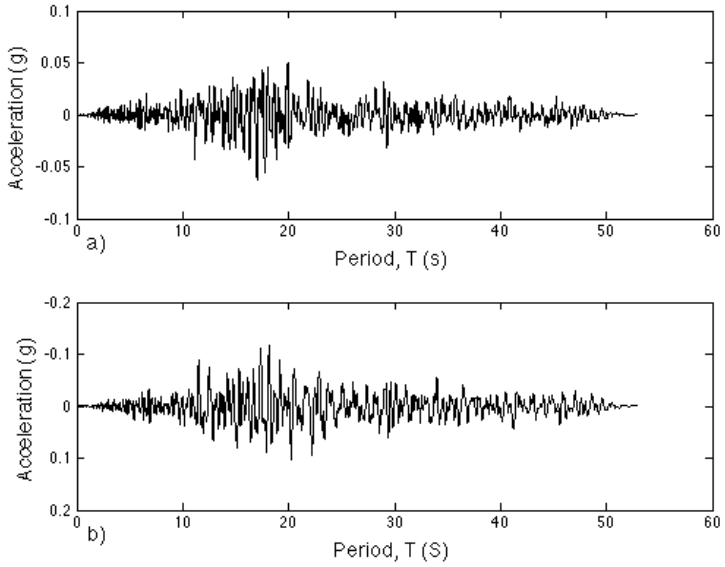

Figure A3. Acceleration time history a) over bedrock b) over soil layer for the November 23th, 1980 Irpinia, Italy-01earthquake (Record sequence No of 293.)

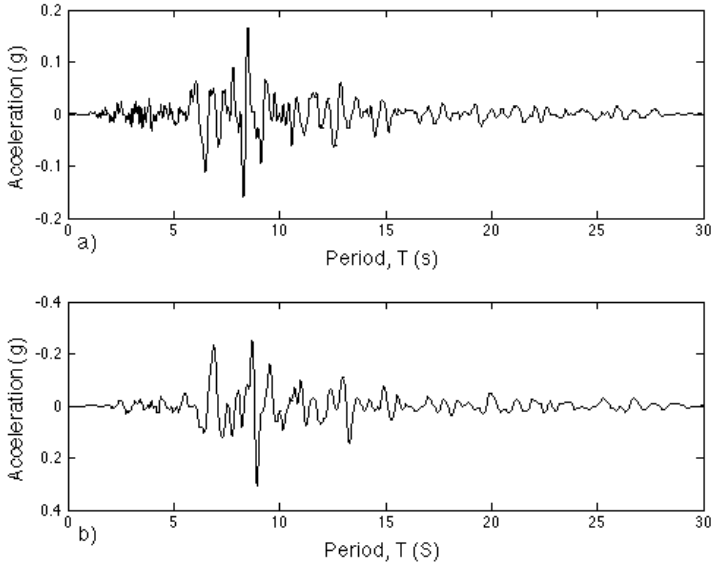

Figure A4. Acceleration time history a) over bedrock b) over soil layer the May 2th 1980 Coalinga-01earthquake (Record sequence No of 369.)

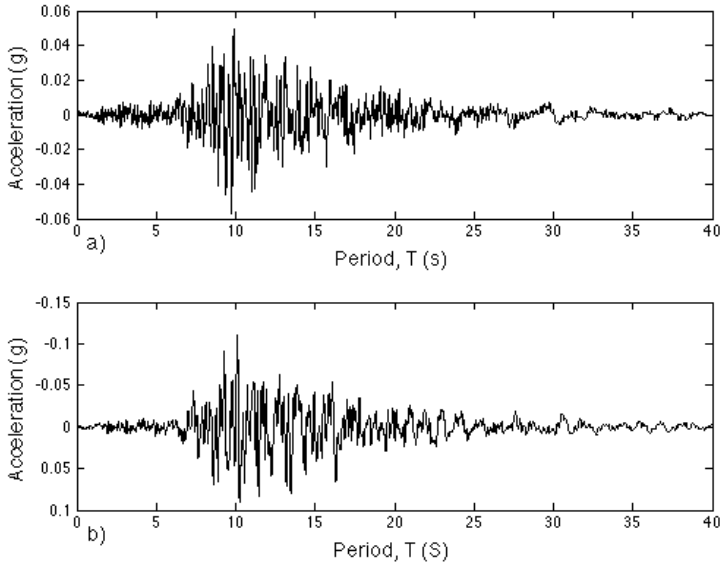

Figure A5. Acceleration time history a) over bedrock b) over soil layer for the October 18th , 1989 Loma Pierta earthquake (Record sequence No of 781.)

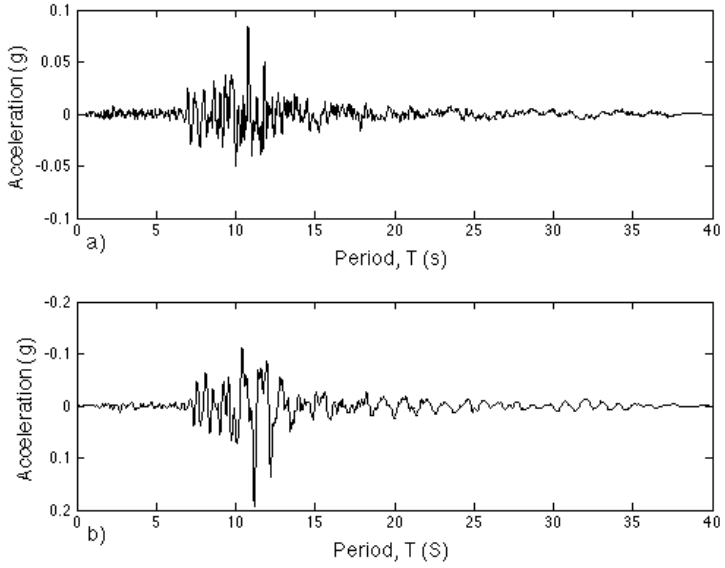

Figure A6. Acceleration time history a) over bedrock b) over soil layer for the October 18th , 1989 Loma Pierta earthquake (Record sequence No of 788.)

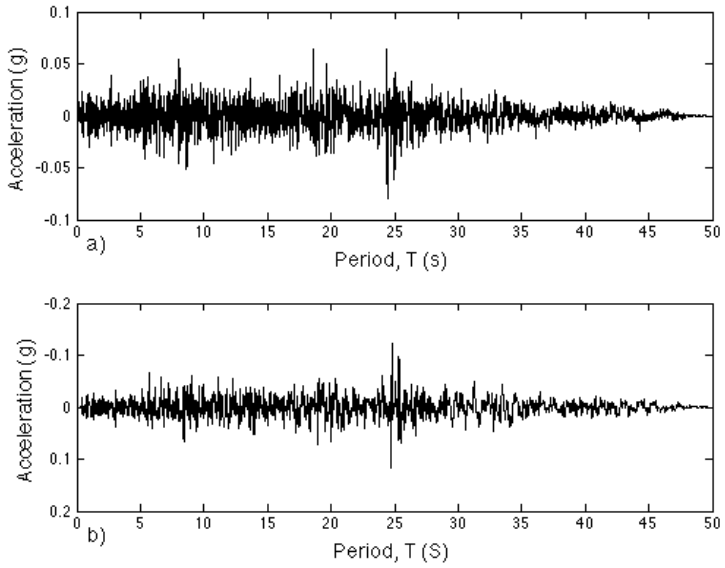

Figure A7. Acceleration time history a) over bedrock b) over soil layer for the June 28th , 1989 Landers earthquake (Record sequence No of 897.)

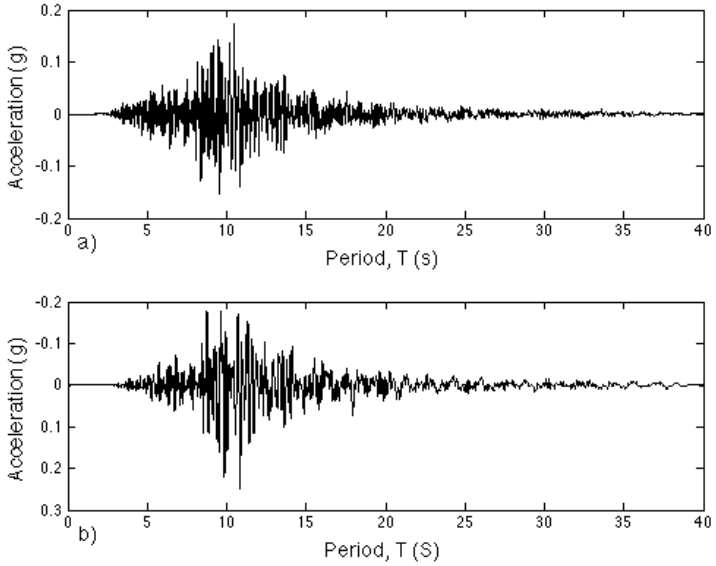

Figure A8. Acceleration time history a) over bedrock b) over soil layer for the January 17th , 1994 Northridge earthquake (Record sequence No of 1020.)

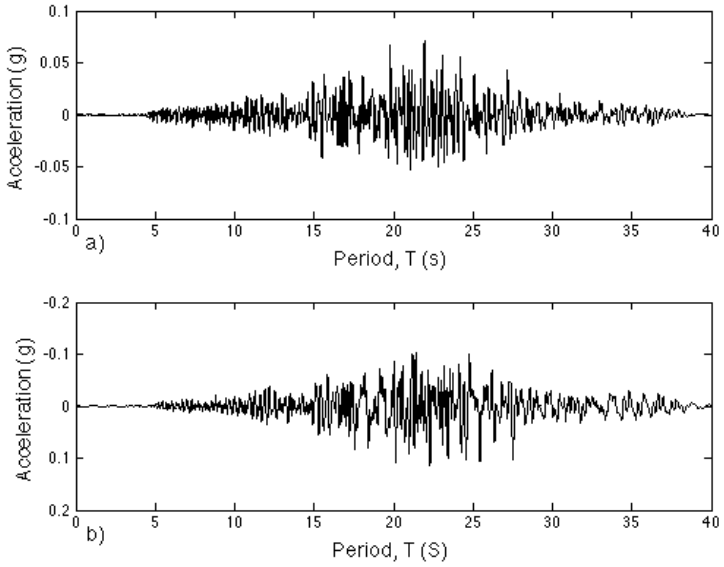

Figure A9. Acceleration time history a) over bedrock b) over soil layer for the January 17th ,1989 Northridge earthquake (Record sequence No of 1060.)

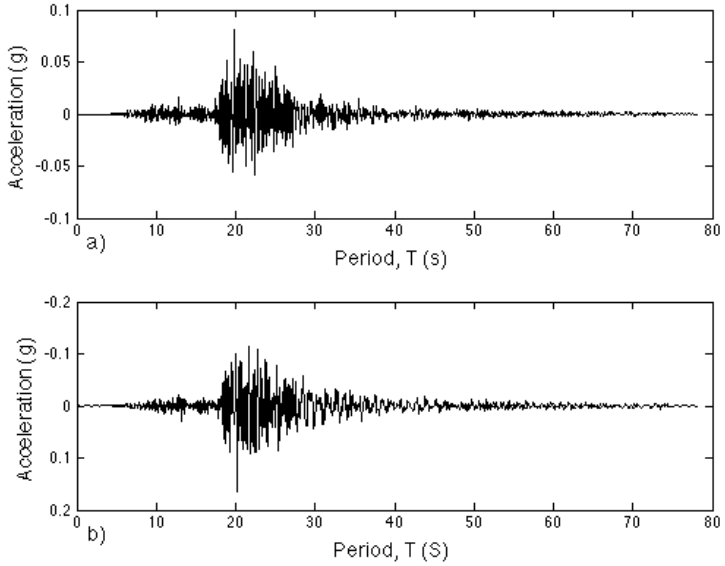

Figure A10. Acceleration time history a) over bedrock b) over soil layer for the January 16th ,1995 Kobe, Japan earthquake (Record sequence No of 1112.)

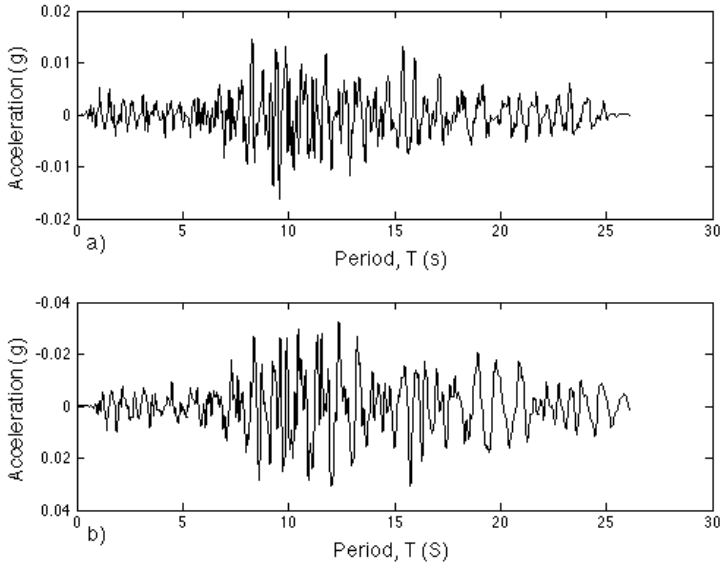

Figure A11. Acceleration time history a) over bedrock b) over soil layer for the May 13th 1995 Kozani, Greece-01 earthquake (Record sequence No of 1125.)

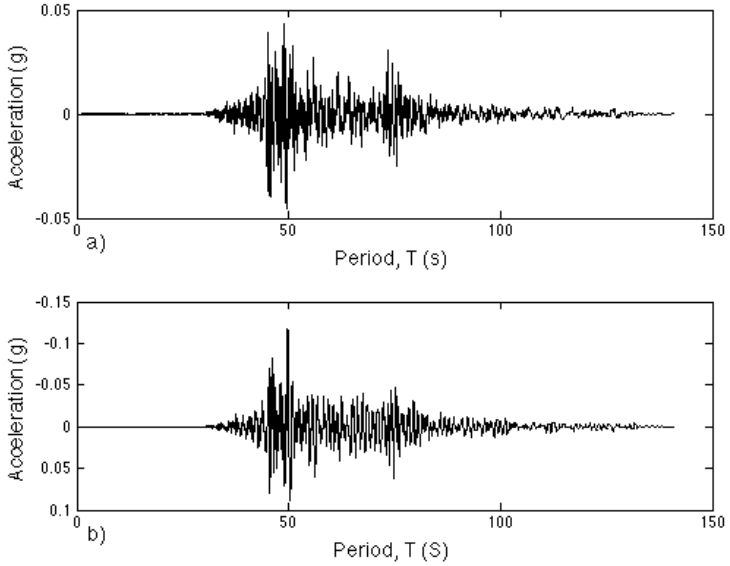

Figure A12. Acceleration time history a) over bedrock b) over soil layer for the August 17th , 1999 Kocaeli, Turkey earthquake (Record sequence No of 1154.)

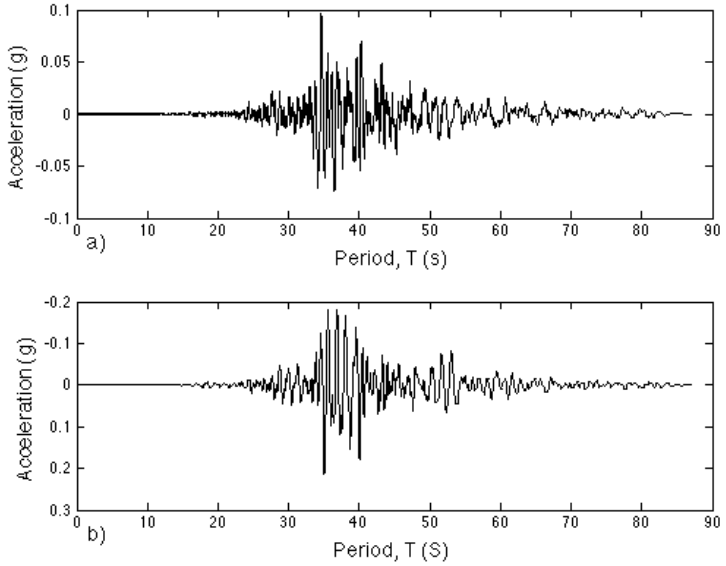

Figure A13. Acceleration time history a) over bedrock b) over soil layer for the September 20th , 1999 Chi-Chi, Taiwan earthquake (Record sequence No of 1278.)

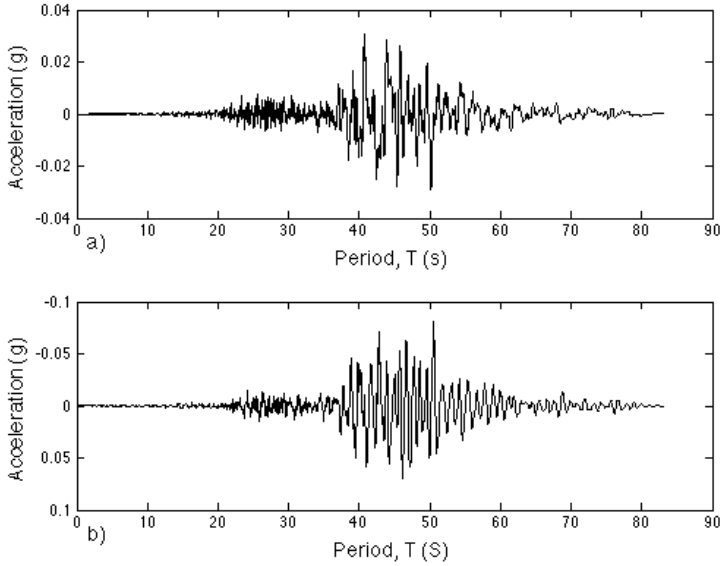

Figure A14. Acceleration time history a) over bedrock b) over soil layer for the September 20th , 1999 Chi-Chi, Taiwan earthquake (Record sequence No of 1446.)

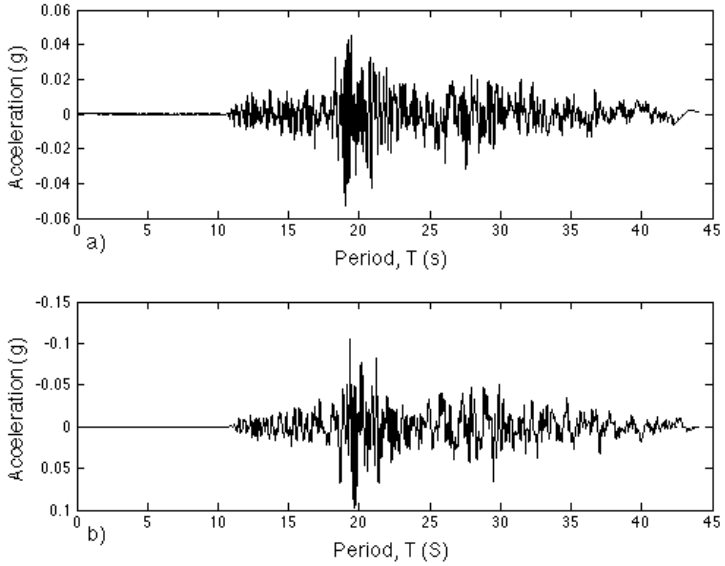

Figure A15. Acceleration time history a) over bedrock b) over soil layer for the November 12th , 1999 Duzce, Turkey earthquake (Record sequence No of 1613.)

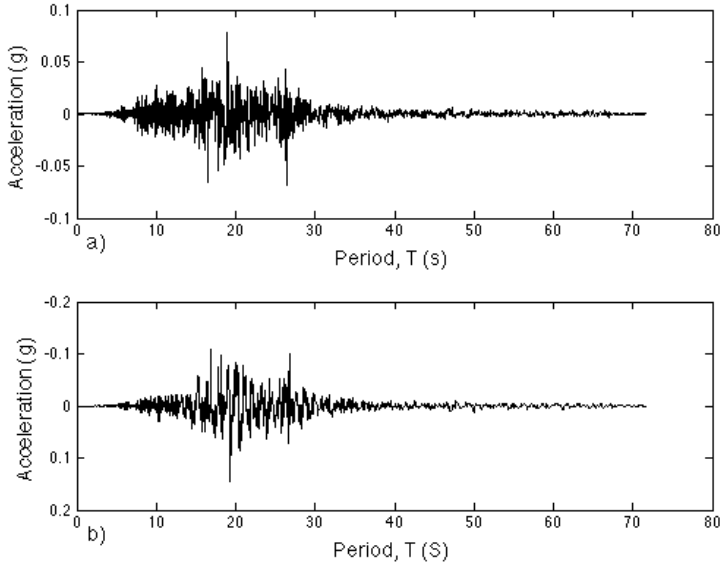

Figure A16. Acceleration time history a) over bedrock b) over soil layer for the October 16th , 1999 Hector Mine earthquake (Record sequence No of 1795.)

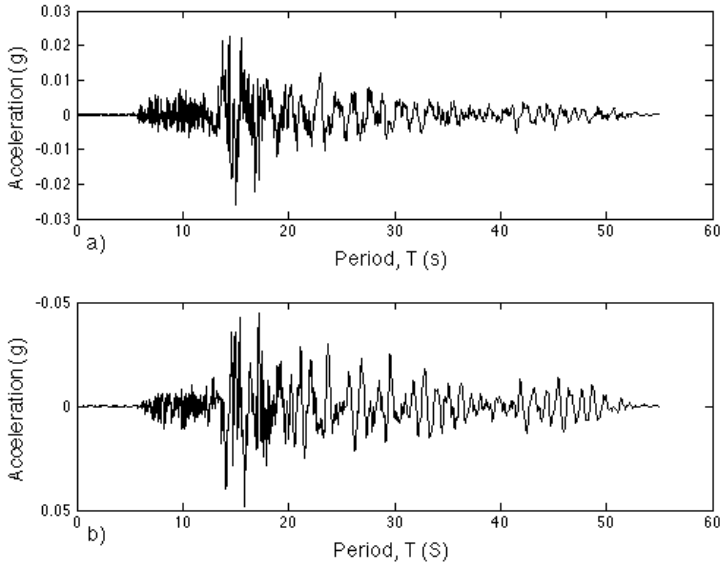

Figure A17. Acceleration time history a) over bedrock b) over soil layer for the September 25th , 1999 Chi-Chi, Taiwan-06 earthquake (Record sequence No of 3350.)

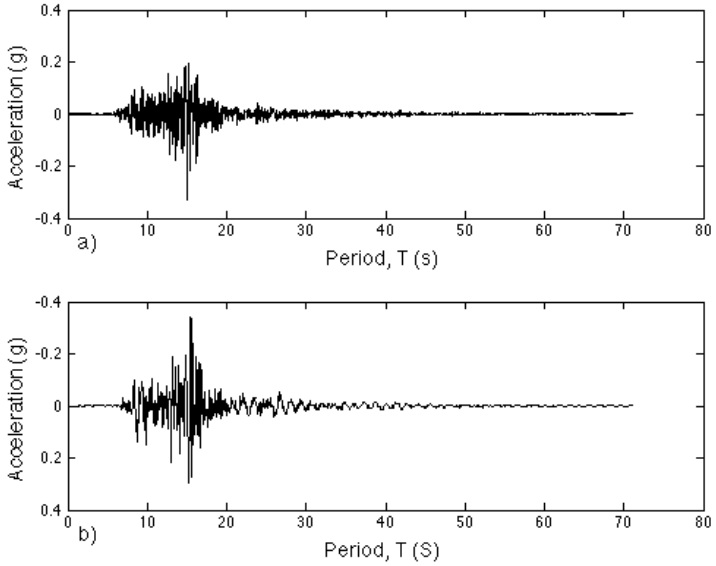

Figure A18. Acceleration time history a) over bedrock b) over soil layer for the September 25th Chi-Chi, Taiwan-06 earthquake (Record sequence No of 3507.)

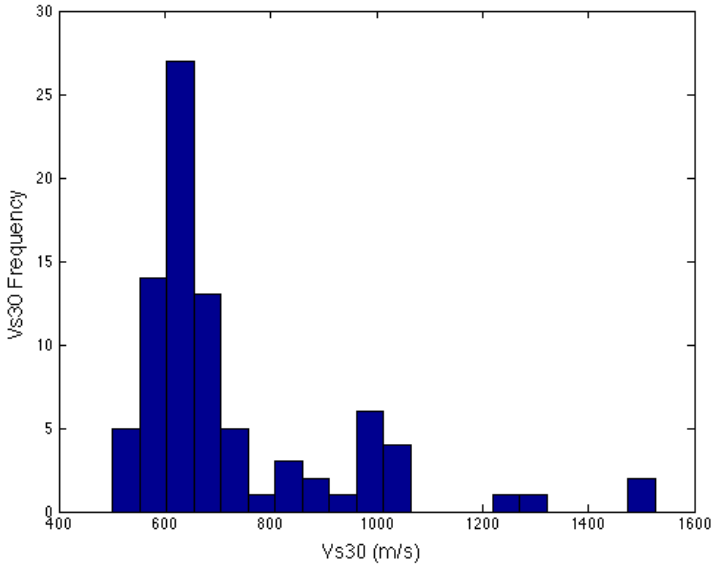

Figure A19. Vs_{30} histogram for the 85 ground motions.

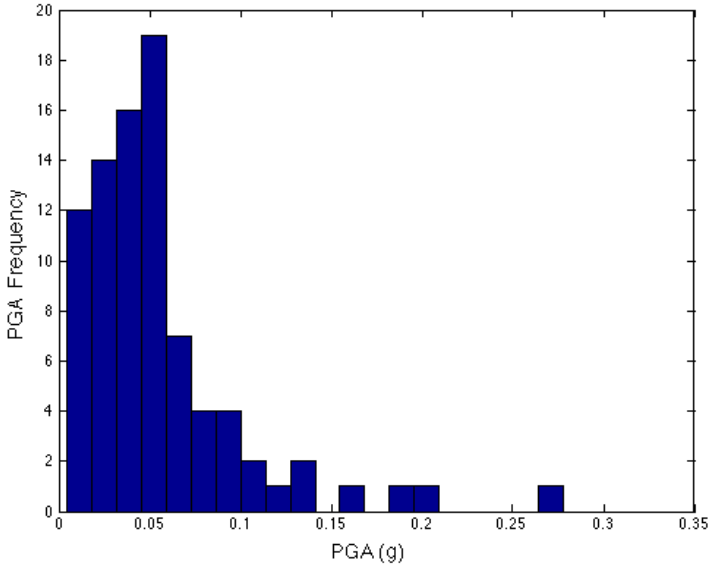

Figure A20. Peak ground acceleration (PGA) histogram for the 85 ground motions.

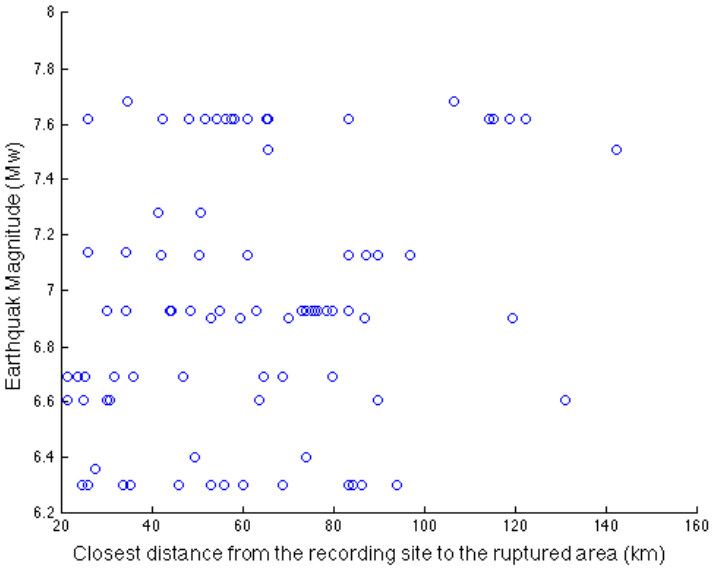

Figure A21. Earthquake Magnitude (Mw) versus Closest distance from the recording site to the ruptured area -ClstD (km) for the 85 ground motions.

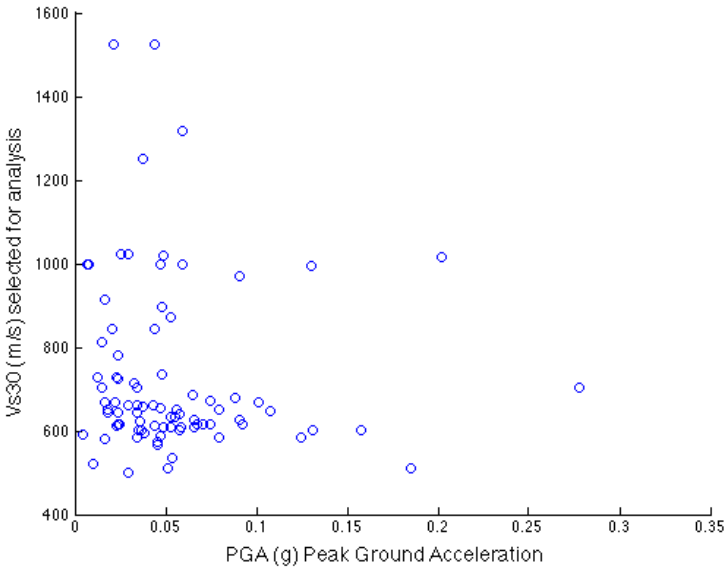

Figure A22. Vs_{30} versus Peak ground acceleration – PGA (g) for the 85 ground motions.